Free Flow Discharge Characteristics of Throatless Flumes

Dev Anand Aukle

A Thesis

in

The Faculty

of

Engineering

Presented in Partial Fulfillment of the Requirements
for the degree of Master of Engineering at
Concordia University
Montréal, Québec, Canada

December 1983

ABSTRACT

FREE FLOW DISCHARGE CHARACTERISTICS OF THROATLESS FLUMES

Dev A. Aukle

A theoretical and experimental analysis of the free flow discharge characteristics of the throatless flume is presented. A pressure correction factor which accounts for the non-hydrostatic pressure distribution at the throat is determined experimentally, and incorporated in the free flow discharge equation developed from energy principles. Tests were conducted on three geometrically similar throatless flumes. Discharges computed from the equation developed show very good agreement with experimental values. An alternate free flow discharge relationship which is simple for computational purposes is approximated from the free flow discharge equation developed. This alternative equation also shows a good agreement with experiments. A limited amount of tests were also carried out to determine the value of the modular limit for the flume. A modular limit of 80% is suggested for flows with flow depth to channel width ratios equal to or less than two.

ACKNOWLEDGEMENTS

I would like to express my thanks to Dr. A.S. Ramamurthy for suggesting the topic and for his guidance in the course of the investigation. I also wish to express my profound sense of gratitude to Dr. M.V.J. Rao for his invaluable guidance and understanding.

I gratefully acknowledge the assistance of Messrs. Louis Stankevicius, Jean Claude Gladu and staff members of the machine shop in the preparation of the experimental set-up.

I would also like to thank the Canadian Commonwealth Scholarship Committee for the funds provided during the years 1981-83.

Last, but not least, I would like to dedicate this work to my wife, Medha, as a remembrance of our academic years in Montréal.

TABLE OF CONTENTS

LIST OF TABLES

Tables

LIST OF FIGURES

NOTATION

B - width at flow section considered

dA - elementary area of flow at a section

E - specified energy

F - Froude number

g - acceleration due to gravity

h - floor pressure

K - pressure distribution coefficient

L_1 - length of converging reach of flume

L_2 - length of diverging reach of flume

L - total length of flume

m, m' - constants

p - pressure at any point within a flow section

q - discharge per unit width

Q - total discharge

V - mean velocity

x - throat width to approach width ratio, B_t/B_1

x_a - width at section a to approach channel width ratio, B_a/B_1

y - flow depth

y_c - critical depth

y'_1 - upstream depth in modular limit studies

z - ordinate of any stream-tube measured from bed

Z - height of hump at throat

α - energy coefficient

α' - pressure correction coefficient

γ - specific weight of water

Note: Subscripts 1, a, t indicate the approach section, section a, and throat section respectively, where the variable is considered, unless otherwise specified in the notation.

CHAPTER 1

-INTRODUCTION

1. INTRODUCTION

1.1 General Remarks

An essential aspect of water resources management is the determination of flow rates in open channels. The most widely used devices to measure flow rates in such open channels, especially in irrigation channels, are the critical-depth flumes. In these flumes, critical depth occurs at a constricted section called the throat which acts as a control. Consequently there is a unique relationship between the water level measured upstream of the throat and the discharge. Among the many critical-depth flumes developed (table 1), the most common one is the Parshall flume (17,18).

One of the recent developments in measuring flumes is the throatless flume (21). This flume has a level floor, a converging inlet section, a diverging outlet section, but unlike conventional venturiflumes, it has no throat. For this reason it was named as the Cut-throat Flume (21) or throatless flume (4). The advantages claimed (22) for this flume are the following: (i) it operates well under both free flow and submerged flow conditions (ii) it has a low head loss because of its level floor (iii) it is very simple in design, and hence very economical.

A simple stage-discharge relationship is very valuable to any field personnel using a measuring device. The stage discharge relationships of throatless flumes developed by earlier investigators are purely empirical, and in the present study a simple discharge equation for rectangular cut-throat flumes under free flow conditions is developed and verified.

1.2 Previous Studies

Skogerboe and Hyatt (21) tested rectangular throatless flumes having identical lengths of converging and diverging sections. The only varying dimension was the width of the throat, W, which was also referred to as the flume size. Flume sizes of 1, 2, 3, 4 and 6 ft were studied under free flow and submerged flow conditions. Based on their studies, they suggested a free flow discharge relation,

$$Q = 3.50\, W^{1.025}\, h_a^{1.56} \qquad \ldots (1)$$

where Q is the flow rate in cfs

and h_a is the piezometric head at section a-a within the converging reach of the flume.

The flumes tested were not geometrically similar.

In a subsequent study, Bennett (3) and Skogerboe et al (22) worked on groups of flumes which were geometrically similar. Based on their experimental study, they suggested the free flow discharge equation,

$$Q = C\, h_a^{n_1} \qquad \ldots (2)$$

where the free flow exponent n_1 is dependent on the flume length, and is constant for a given flume length. The flow coefficient, C, is correlated with throat width, W, for a given flume length as

$$C = K\, W^{1.025} \qquad \ldots (3)$$

where K, is a coefficient which depends on flume length.

Though the flumes were reported to be geometrically similar, the entrance conditions (ratio of channel width to throat width) were not. Keller (12) rightly points out this aspect, and in his work he used geometrically similar flumes and concluded that the effect of non-similarity of the entrance conditions contributed to different discharge relation curves reported in the works of Bennet (3) and Skogerboe et al (22).

Keller noted that another factor of importance was the positioning of the piezometer tapping, which in the earlier study, was positioned in the side wall at an unstated height. The positioning too needed proper scaling as the pressure variation within the converging reach is non-hydrostatic. He placed the pressure tapping at an equal distance from the throat section as in the earlier study, but inserted it in the channel bed. The entrance conditions for the flumes he tested were geometrically similar.

He plotted the results of Skogerboe et al (22) in the non-dimensional form $\frac{Q}{\sqrt{g}\, B_t\, h_a^{1.5}}$ against h_a/B_t and compared the plot with that of his own experimental data. He reported the absence of scale effects.

1.3 Need for the Present Study.

The free flow discharge relations developed in the previous studies (3, 22) involve the use of two coefficients and one exponent to be obtained by extrapolation of the curves presented. Since the flumes were not operating under dynamically similar conditions, the results are limited in applications to widths of the flumes tested. It may be added

that Parshall flumes too have a similar restriction.

Even if one wants to use Keller's discharge relation curve (12), one needs the measurement of h_a, the bottom pressure reading located within the converging section at one third the distance from entry to throat. This measurement is influenced by curvature of the streamlines in the converging reach of the flume. Experiments show that the ratio of h_a to the actual depth y_a decreases with increasing flow rates (fig. 1). It is also difficult to install the bottom tap in existing channels, and it is liable to get clogged.

Under field conditions, it would be ideal to use a discharge relation involving a single measurement such as depth in the approach channel where the flow is not influenced by curvature effects. The present study aims at developing such a discharge equation for the conditions of free flow in thrpatless flumes. The energy approach is used to develop a discharge equation. Experiments were conducted on three geometrically similar flumes to verify the equation developed.

CHAPTER 2

THEORETICAL CONSIDERATIONS

2. THEORETICAL CONSIDERATIONS

2.1. Development of the Free Flow Discharge Equation

The following assumptions are made in the relationships linking the discharge rate, Q, with approach flow depth, y_1, and the geometrical parameters of the flume:

(i) the cross-section of the flume is rectangular, and the floor is horizontal;

(ii) the approach flow is sub-critical;

(iii) head losses in the short converging reach are negligible;

(iv) the rate of discharge at the throat section is maximum (fig.2)

A definition sketch of the throatless flume is given in Fig. 3.

The specific energy across the throat section is given by

$$E_t = \alpha_t' y_t + \alpha_t \frac{v^2}{2g}$$

$$= \alpha_t' y_t + \alpha_t \frac{Q^2}{2g B_t^2 y_t^2} \quad \ldots\ (4)$$

In the converging reach of the flume, the flow is accelerating, and hence the velocity distribution will be nearly uniform. This has also been verified experimentally (fig. 4). Therefore $\alpha_t = 1$.

The coefficient α_t' which takes care of pressure variations in the flow at the throat section is given by

$$\alpha_t' = \frac{1}{Qy} \int \left(\frac{p}{\gamma} + z\right) v \, dA \qquad \ldots (5)$$

where y = hydrostatic depth at a point (x,z)

p = pressure at any point (x,z)

z = ordinate of any streamtube measured from the bed.

Based on the experimental observations, the pressure at the throat is approximated by a linear function of the depth (fig. 5)

i.e. $$\frac{p}{\gamma} = K \quad y \qquad \ldots (6)$$

Substituting equation (6) and $z = y_t - y$ in equation (5), one obtains

$$\alpha_t' = \frac{1}{Qy_t} \int_o^{y_t} (Ky + y_t - y) \, v \, dA \qquad \ldots (7)$$

Considering unit-width of flow, then $Q = q$, $v = q/y_t$ and $dA = dy$, and equation (7) reduces to

$$\alpha_t' = \frac{K + 1}{2} \qquad \ldots (8)$$

A similar result was quoted by Nasser et al (15) relating pressure coefficient, α', with force coefficient, β'.

Combining equations (4) and (8), yields

$$E_t = \left(\frac{1 + K}{2}\right) y_t + \frac{Q^2}{2gB_t^2 y_t^2} \qquad \ldots (9)$$

The flumes tested were geometrically similar, hence K may be expressed as a function of y_t/B_t only:

$$K = f\,(y_t/B_t) \qquad \ldots (10a)$$

Experimentally it was found that the relationship of K to y_t/B_t can be approximated by a linear equation of the type

$$K = 1 - m'(y_t/B_t) \qquad \ldots (10b)$$

where $m' = 0.173$, an empirical constant for the range of test parameters (fig. 6).

After substituting eq. (10b) in eq. (9), it can be re-written in the following form:

$$q_t^2 = 2g\, y_t^2 \left[E_t - \frac{[2 - m'(y_t/B_t)]}{2}\, y_t\right] \qquad \ldots (11)$$

One can obtain the condition for maximum discharge (Specific energy being constant) by differentiating q_t w.r.t. y_t in eq. (11) and equating it to zero. This results in

$$y_t^3 = \frac{Q^2}{K\, g\, B_t^2} \qquad \ldots (12)$$

Owing to the difficulty of depth measurement at the throat and the fact that a relationship in terms of upstream depth, y_1, is desired, the experimental K values have been related to y_1/B_1; further it is observed that a better linear fit is obtained compared to the variation of K with y_t/B_t. The linear fit is found to follow the relationship

$$K = 1 - m\left(\frac{y_1}{B_1}\right) \qquad \ldots (13)$$

where the constant, m = 0.29, for the range of test parameters (fig. 7).

The Specific energy at the upstream section (1) can be written as

$$E_1 = \alpha_1 y_1 + \alpha_1 \frac{V_1^2}{2g} \qquad \ldots (14)$$

Both α_1 and α_1 can be taken as equal to unity since the flow in section (1) is uniform. Thus

$$E_1 = y_1 + \frac{V_1^2}{2g}$$

$$= y_1 + \frac{Q^2}{2g\, B_1^2\, y_1^2} \qquad \ldots (15)$$

Equating E_1 to E_t, one obtains

$$y_1 + \frac{Q^2}{2g\, B_1^2\, y_1^2} = \alpha_t y_t + \frac{Q^2}{2g\, B_t^2\, y_t^2} \qquad \ldots (16)$$

Substituting for y_t and α_t from equations (12) and (8) respectively, and simplifying, one obtains,

$$\left(\frac{Q^2}{g\, B_1^5}\right)^{1/3} = \frac{2\, K^{1/3}\, x^{2/3}}{(1 + 2K)} \left[\frac{y_1}{B_1} + \frac{Q^2}{2g\, B_1^5} \left(\frac{B_1}{y_1}\right)^2\right] \qquad \ldots (17)$$

where $$x = B_t/B_1 \qquad \ldots (18)$$

In equation (17), x is a constant for the flumes tested, and K is dependent on y_1/B_1 (vide eq. 13). For assumed values of y_1/B_1,

equation (17) can hence be solved for $\frac{Q^2}{g B_1^5}$. The discharge relationship is plotted in fig. 8.

2.2 Variation of y_t/y_1 with y_1/B_1

By suitable manipulation, equation (17) may be expressed as a polynomial in terms of y_t/y_1:

$$\frac{K}{2} x^2 \left(\frac{y_t}{y_1}\right)^3 - \left(\frac{1 + 2K}{2}\right) \frac{y_t}{y_1} + 1 = 0 \qquad \ldots (19)$$

For a given flume, the above equation can be solved for y_t/y_1 for assumed values of y_1/B_1 alone, since K is also a function of y_1/B_1.

The variation of y_t/y_1 with y_1/B_1 is shown in fig. 9.

The value of y_t/y_1 corresponding to a particular y_1/B_1 can be substituted in equation (12) to obtain the flow rate, Q.

2.3 Alternate Discharge Relationship:

In the field, the depth to width ratios (y_1/B_1) encountered are usually less than two. An approximate linear relationship (applicable in the above range of y_1/B_1) can be developed for the dependence of y_t/y_1 on y_1/B_1 (fig. 9):

$$\frac{y_t}{y_1} = 0.67 + 0.24 \, (y_1/B_1) \qquad \ldots (20)$$

From equations 12, 13, 20, the following discharge relation can be derived

$$\frac{Q^2}{g B_1^5} = x^2 \left[1 - 0.29 \left(\frac{y_1}{B_1}\right)\right] \left\{ \left(\frac{y_1}{B_1}\right) \left[0.67 + 0.24 \left(\frac{y_1}{B_1}\right)\right]\right\}^3 \quad \ldots (21)$$

The above equation is simpler than equation (17) for computation of Q. The discharges computed using eq. (21) are plotted against experimental discharges in fig. 10.

2.4 The Discharge Relationship Expressed in terms of h_a, the floor pressure measured at Section a

Using a similar approach as in section 2.1, one obtains

$$E_t = E_a$$

or
$$\alpha_t y_t + \frac{Q^2}{2g B_t^2 y_t^2} = \alpha_a y_a + \frac{Q^2}{2g B_a^2 y_a^2} \quad \ldots (22)$$

where
$$\alpha_a = \frac{1 + K_a}{2} \quad \ldots (23)$$

Combining equations (8), (12), (22), (23), one obtains

$$\left(\frac{1 + 2K}{2K^{1/3}}\right) \left(\frac{Q^2}{g B_t^2 h_a^3}\right)^{1/3} = \left[\frac{1 + K_a}{2K_a} + \frac{(K_a x_a)^2}{2}\right] \frac{Q^2}{g B_t^2 h_a^3} \quad \ldots (24)$$

K and K_a are expressed in terms of h_a/B_t by means of empirically obtained relationships (fig. 11 and fig. 12), which are approximated by the linear equations:

$$K_a = 1 - 0.035\ (h_a/B_t) \quad \ldots (25)$$

and

$$K = 1 - 0.165\ (h_a/B_t) \quad \ldots (26)$$

For any value of h_a/B_t, equation (24) can be solved to obtain $\frac{Q}{\sqrt{g}\ B_t\ h_a^{1.5}}$, and hence the flow rate Q, Fig. 13 shows the variation of $\frac{Q}{\sqrt{g}\ B_t\ h_a^{1.5}}$ with h_a/B_t.

CHAPTER 3

EXPERIMENTAL SET-UP AND PROCEDURE

3. Experimental Set-up and Procedure

A schematic layout of the experimental set-up is shown in fig. 14. Three geometrically similar rectangular throatless flumes were built using half-inch thick plexiglass sheets. The dimensions of the flumes are given in Fig. 15.

The tests were performed in an 18.5" deep glass-walled horizontal channel. The approach and exit channels had widths matching with the test flume width (fig. 14). Sufficient taps were provided to measure floor pressures (fig. 14). A static pressure probe with flat horizontal limb was used to record the static pressure distribution. A pitot tube was used to obtain velocity profiles.

Flow depths and surface profiles were measured by means of point gauges which had an accuracy of 0.001 ft and the discharge was measured with the help of a standard 60° V-Notch. The accuracy of measurements are summarised in Table 2.

Water was pumped from a sump through a 10 in. diameter pipeline. The water was dropping vertically into the entrance region of the test channel. The control valve on the pipeline was set for each test, and the tailgate at the downstream end of the channel was kept fully open to ensure free flow conditions. For the modular limit studies, the tailgate was raised in increments, and measurements were repeated for each increment.

CHAPTER 4

ANALYSIS OF RESULTS

4. ANALYSIS OF RESULTS

4.1 Experimental Results:

4.1.1 Flow Surface Profiles and Floor Pressure Profiles

The flow surface profiles for some of the tests conducted are shown in fig. 16. The floor pressure profiles for the same tests are shown in fig. 17. Fig. 18 shows both the floor pressure profile and surface profile for selected discharge rates.

At the entry of the flume, the floor pressure and surface profiles are close to each other. As the flow progresses downstream, the curvature of the surface profile becomes more and more pronounced. Consequently the two profiles diverge from each other upto a section close to the throat.

The floor pressure becomes equal to the flow depth at a section downstream of the throat. This section appears to be the point of inflexion. This point was found to move further downstream from the throat with increasing flow rates. The pressure distribution across this section was measured to check the nature of distribution. It was observed that there was a noticeable deviation from hydrostatic distribution near the surface. The measured depth at the section was found to be less than critical depth based on uniform flow $\left[y_c^3 = \frac{Q^2}{g B^2}\right]$.

4.1.2 Pressure Distribution at the Throat

The pressure distribution across the throat section was studied for a wide range of discharges. This distribution was essentially uniform across any horizontal section. Hence the pressure distribution was recorded only at the centre of the throat (fig. 5).

The pressure distribution was found to deviate from hydrostatic. The actual distribution curve is approximated by a straight line which ensures zero pressure at the free surface and the total pressure force equal the measured value (fig. 5). The piezometric head at any point in the throat section is thus expressed as in eq. (6).

Fig. 5 shows the values of K obtained from the experiments. It may be observed that K decreases with increasing flow rates.

The K values when plotted against y_t/B_t and y_1/B_1 ratios were found to follow approximate linear relationships. (Eqs (10b) and (13), figs. 6, 7).

4.1.3 Pressure Distribution at Section a

The pressure distribution at section-a was also recorded and the resulting analysis indicated that the pressure distribution, which was almost linear, can be approximated by the equation

$$\frac{p}{\gamma} = K_a\, y \qquad \ldots (27)$$

The K_a values are plotted against h_a/B_t (fig. 12).

4.2 The Free-flow Discharge Equation

A discharge relationship derived on the basis of the energy principle with α_t taken equal to one was giving erroneous results. For any discharge, the calculated critical depth $[y_c^3 = Q^2/g\ B_t^2]$ was found to be less than the actual measured depth at the throat (Tables 3, 4, 5), the deviation being larger with increasing flow rates. This can be attributed to the non-hydrostatic nature of the pressure distribution at the throat.

The relationship between K and y_1/B_1 (fig. 7) was used to develop eq. (17) and fig. 8, which indicates the dependence of $\frac{Q}{g\ B_1^5}$ on y_1/B_1. In the range of the experimental studies (y_1/B_1 upto 2), the flow rates obtained for the above discharge equation agree very closely with measured flow rates. As stated earlier, the depth to width ratios (y_1/B_1) encountered in irrigation channels are usually zero to 2, which is also the range covered in this study.

4.3 Alternate Free Flow Discharge Equation

Eq. (21) provides an explicit approximate relationship between Q and y_1/B_1. Hence it is simpler to use eq. (21) compared to eq. (17).

The discharges computed using eq. (21) are plotted against the corresponding measured discharges in fig. 10. From this figure, it may be observed that a good agreement exists. However, when a higher degree of accuracy is required, eq. (17) is recommended.

4.4 Comparison with Previous Studies

The discharge relationship obtained in terms of h_a/B_t (eq. (24) and fig. 13) shows good agreement with the data of the present study and with those of the previous study (12).

It can be observed that the curve tends to reach a lower limit of $Q/\sqrt{g}\, B_t\, h_a^{1.5}$, and it would be interesting to investigate its value. With the help of the discharge equation (24), this lower limit can be derived as follows:

For low values of h_a/B_t, both K and K_a tend to 1. Eq. (24) then becomes

$$\frac{3}{2} M^{1/3} = 1 + \frac{x_a^2}{2} M \qquad \ldots (28)$$

where

$$M = \frac{Q^2}{g\, B_t^2\, h_a^3} \qquad \ldots (29)$$

and $x_a = B_t/B_a = 0.619$ for all the datas shown in fig. 13. Inserting the value of x_a in eq. (28) and solving for M results in the value of $Q/\sqrt{g}\, B\, h_a^{1.5} = 0.602$, which is in good agreement with the observed trend in fig. 13.

At this stage, it would be interesting to investigate the behaviour of a similar relationship as in fig. 13, but in terms of the upstream depth, y_1, instead of h_a. Eq. (17) can be re-arranged to obtain the following equation:

$$\left(\frac{1 + 2K}{2}\right) \left(\frac{Q^2}{g\, B_t^2\, y_1^3}\right)^{1/3} = K^{1/3} \left[1 + \frac{x^2}{2} \cdot \frac{Q^2}{g\, B_t^2\, y_1^3}\right] \qquad \ldots (30)$$

For low values of y_1/B_t, K tends to 1, and eq. (30) reduces to the form

$$1.5\ N^{1/3} = 1 + \frac{x^2}{2}\ N \qquad \ldots (31)$$

where $$N = \frac{Q^2}{g\ B_t y_1^3}$$

and $x = B_t/B_1 = 0.52$ for the flumes tested.

Inserting the value of x in eq. (31) and solving for N results in the value of $Q/\sqrt{g}\ B_t\ y_1^{1.5} = 0.582$, which is in good agreement with the observed trend shown in fig. 19.

One may investigate whether there is an upper limit to the value of $Q/\sqrt{g}\ B_t\ y_1^{1.5}$ by writing the expression as

$$\frac{Q}{\sqrt{g}\ B_t\ y_1^{1.5}} = \frac{Q}{\sqrt{g}\ B_1\ y_1^{1.5}}\ \frac{B_1}{B_t} = F_1\ \frac{B_1}{B_t} \qquad \ldots (32)$$

where F_1 is the Froude number at section 1.

The theoretical upper limit of the Froude number in the approach channel is 1, and consequently the term $Q/\sqrt{g}\ B_t\ y_1^{1.5}$ will be asymptotic to the value of B_1/B_t, which is equal to 1.923 for the flume geometry used in the study.

4.5 Modular Limit Studies

It is necessary to specify the limit of validity of the free flow theory in the study of any open channel flow measuring device.

When the depth of flow downstream from the flume increases to the point where it just starts to cause the upstream head to increase, the flume is said to be operating at the modular limit (1). Some studies were carried out to establish this limit for the throatless flume.

Based on the study, a modular limit of about 80% is recommended for the application of the free flow equation. This value limits the increase of upstream depth y_1 to within 1%.

Details of the study are presented in Appendix V.

4.6 Effect of Hump

A simple rise in the flume bed termed as a hump is sometimes used to promote the formation of a control section at which the flow depth is uniquely related to the discharge (5, 11).

In the present study, the theoretical energy equation (16) was modified to account for the presence of the hump (see eq. (33) in Appendix VI).

A few tests were conducted to examine the characteristics of flow when a hump was placed in the flume, and to check the validity of the relationship derived. Details of the study are presented in Appendix VI.

CHAPTER 5

CONCLUSIONS AND RECOMMENDATIONS

5. CONCLUSIONS AND RECOMMENDATIONS

5.1 Conclusions

The following conclusions may be drawn from the present study:

(i) A generalised free flow discharge equation is derived for the throatless flume by incorporating the necessary correction factor in the energy equation to account for the non-hydrostatic pressure distribution. The validity of the equation was found to be satisfactory for geometrically similar flumes operating within the range of approach channel depth to width ratio equal to two. The equation is applicable to flumes having throat width to approach channel width ratio equal to 0.52, and having converging length to diverging length ratio equal to 0.5. Based on the limited study carried out to determine the modular limit of these flumes, a modular limit of 80% is recommended to limit the increase in upstream depth to 1%.

(ii) An alternate free flow discharge equation which is simple for computational purposes has been approximated from the relationship developed above. Within the range tested (approach channel depth to approach channel width equal to two) and for the flumes tested (throat width to approach channel width equal to 0.52, and converging length to diverging length ratio equal to 0.5), this explicit equation has a close agreement with measured discharges.

5.2 Scope for further Study

The following further investigations are suggested in order to supplement the present study:

(i) While the range of y_1/B_1 may be satisfactory for most field applications, the study can be extended to cover a larger range of y_1/B_1 in order to check the validity of equation (17) beyond the value of $y_1/B_1 = 2$.

(ii) It would be desirable to work with models having (a) varying entrance width to throat width ratios, and (b) varying converging length to diverging length ratios. The effect of these parameters may be incorporated in the discharge equation, with the aim of obtaining a free flow stage discharge relationship applicable to any geometry of a throatless flume.

(iii) The modular limit has to be established by more extensive studies on these flumes. It is also of practical interest to investigate the flow characteristics under submerged flow conditions.

APPENDIX I

REFERENCES

APPENDIX I - REFERENCES

1. Ackers, P., White, W.R., Perkins, J.A. and Harrison, A.J.M., Weirs and flumes for flow measurement. John Wiley and Sons Ltd. 1978, N.Y.
2. Balloffet, A. 1955, Critical flow meters (Venturi Flumes). Proceedings of the American Society of Civil Engineers, 81 (1955), Paper No. 743, July, pp. 1-31, Ann Arbour, Michigan.
3. Bennett, R.S. 1972, Cut-throat flume discharge relations. Thesis presented to Colorado State University at Fort Collins, Colo. in 1972, in partial fulfillment of the requirements for the degree of Master of Science.
4. Boss, M.G. 1976, Discharge measurement structures. International Institute for Land Reclamation and Improvement/ILRI, Waneringen, 1976. The Netherlands.
5. Chow, V.T., Open-Channel Hydraulics. McGraw-Hill Book Company, New York, 1959.
6. Cone, V.M. 1917, The Venturi Flume. Journal of Agricultural Research, 9 (4): 115-123. April 23, 1917.
7. Engel, F.V.A.E., The Venturiflume, The Engineer, 158, 104 (3 August 1934); 131-133 (10 August 1934).
8. Ferguson, J.E., and Garbon, J.E. 1949, A modified Venturi Section for measuring irrigation water in open channels: Agricultural Engineering, Vol. No. 30, 1949.
9. Henderson, F.M., Open Channel Flow, MacMillan Publishing Co., New York, 1966.

10. Holtan, H.N., Minshall, N.E., and Harrold, L.L. 1962, Field Manual for research in agricultural hydrology. Soil and Water Conservation Research Division, Agricultural Research Service. Agricultural Handbook No. 224.

11. Inglis, C.C. 1928, Notes on standing wave flumes and flume meter falls. Government of Bombay, Public Works Department Technical Paper No. 15.

12. Keller, R.J., 1981, Scale effect in model studies of cut-throat flumes. International Association for Hydraulic Research, Subject D(a), Paper No. 5. XIX Congress, New Delhi, India, 1981.

13. Khafagi, Anwar 1942, Der Venturikanal (Theorie und Anwendung), Zürich 1942. Dis-Druckerei A.G. Gebr. Leeman and Co., Stockerstr. 64.

14. Kruse, E.G. 1964, Trapezoidal flumes for measuring discharges in irrigation channels. Agricultural Research Service, United States Department of Agricultuire, Fort Collins, Colorado, CER64EGK14.

15. Nasser, M.S., Vankataraman, P. Ramamurthy, A.S. 1980, Curvature Corrections in open channel flow, Canadian Journal of Civil Engineering , 7, 421-431. 1980.

16. Osborn, H.B., Keppel, R.V. and Renard, K.G. 1963, Field performance of large critical-depth flumes for measuring runoff from semi-arid rangelands. ARS 41-69, Agricultural Research Service, United States Dept. of Agriculture.

17. Parshall, R.L. 1926, The improved Venturi flume. Proceedings American Society of Civil Engineers, Sept. 1926.

18. Parshall, R.L. 1950, Measuring water in irrigation channels with Parshall flumes and small weirs. Soil Conservation Service Circular No. 843. United States Dept. of Agriculture.

19. Rasheed, M.A. 1968, Hydraulic Characteristics of a modified Venturi section. PRWR 13-12 T, Utah Water Res. Lab, College of Engineering, Utah State Univ., Logan, Utah.

20. Robinson, A.R. and Chamberlain, A.R. 1960, Trapezoidal flumes for open channel flow measurement. Transactions of the American Society of Agricultural Engineers Vol.3, No. 2, Saint Joseph, Michigan.

21. Skogerboe, G.V. and Hyatt, M.L., 1967, Rectangular cut-throat flumes, Jour. Irrig. Drain. Div., ASCE, Vol. 98, No. IR4, pp. 569-583.

22. Skogerboe, G.V., Bennett, R.S. and Walker, W.R. 1972, Generalised discharge relations for cut-throat flumes, Jour. Irrig. Drain. Div. ASCE, Vol. 98, No. 1R4, pp. 569-583.

APPENDIX II

FIGURES

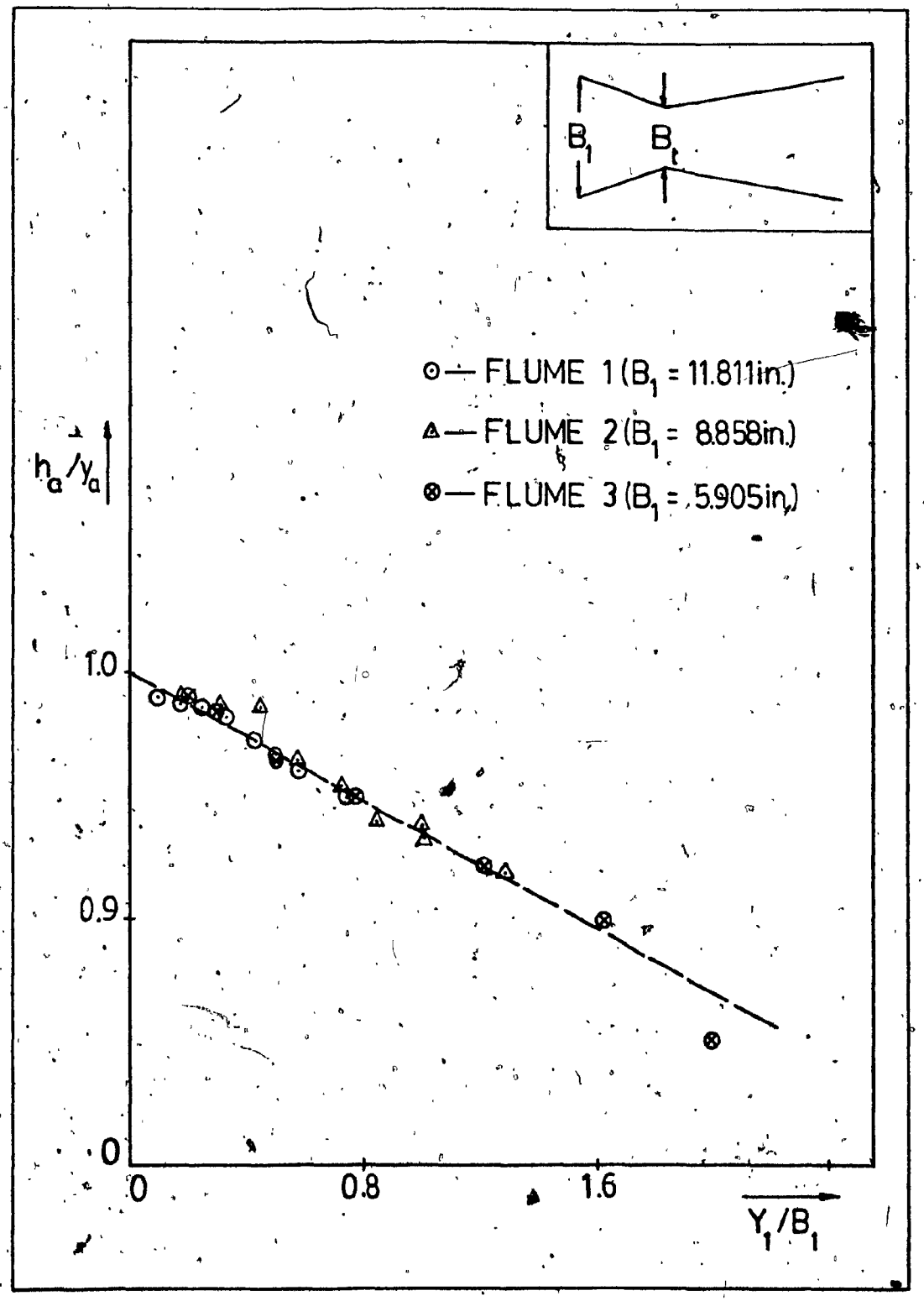

FIG. 1. VARIATION OF h_a/y_a WITH y_1/B_1.

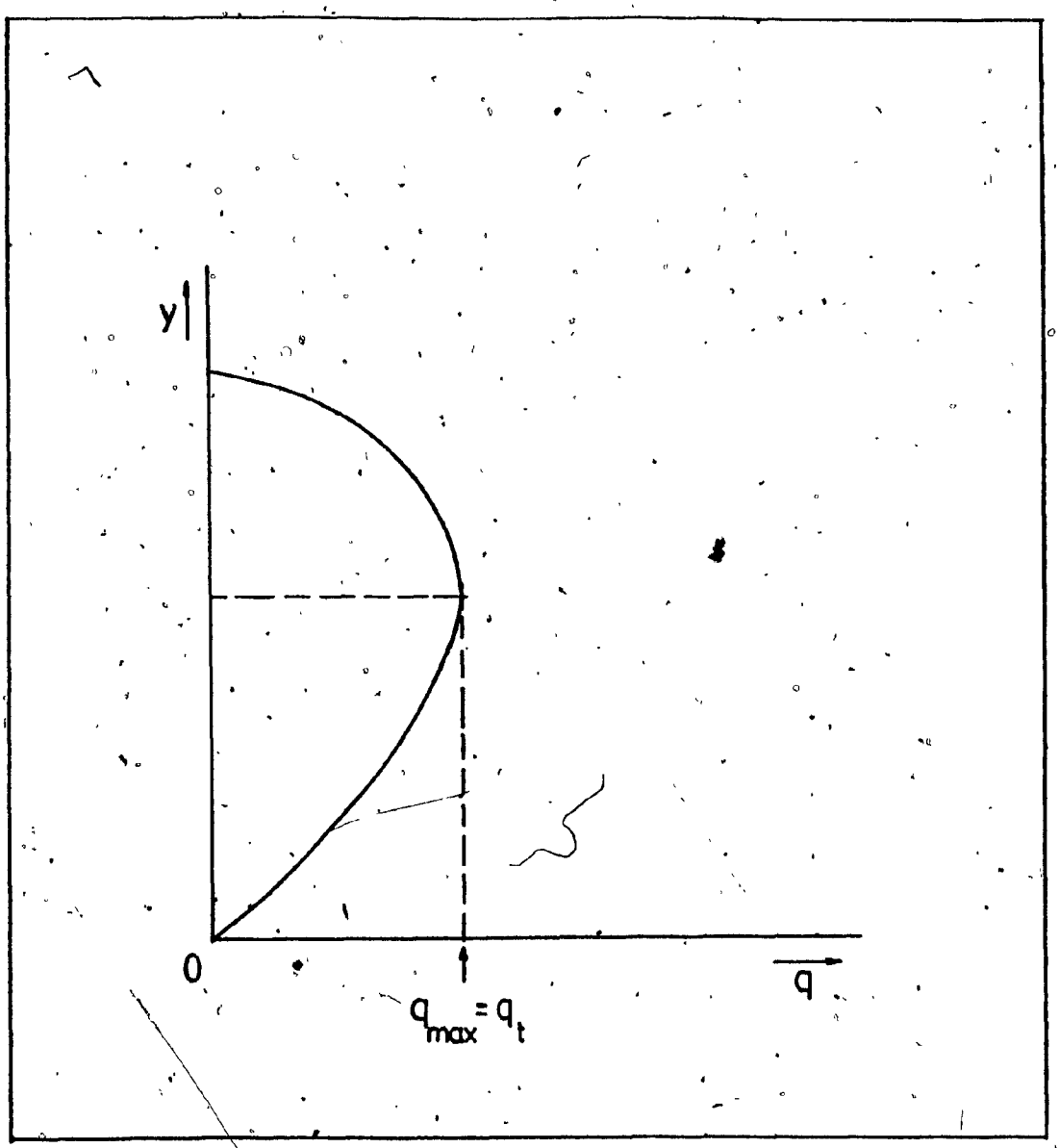

FIG. 2. DISCHARGE-DEPTH CURVE FOR CONSTANT SPECIFIC ENERGY.

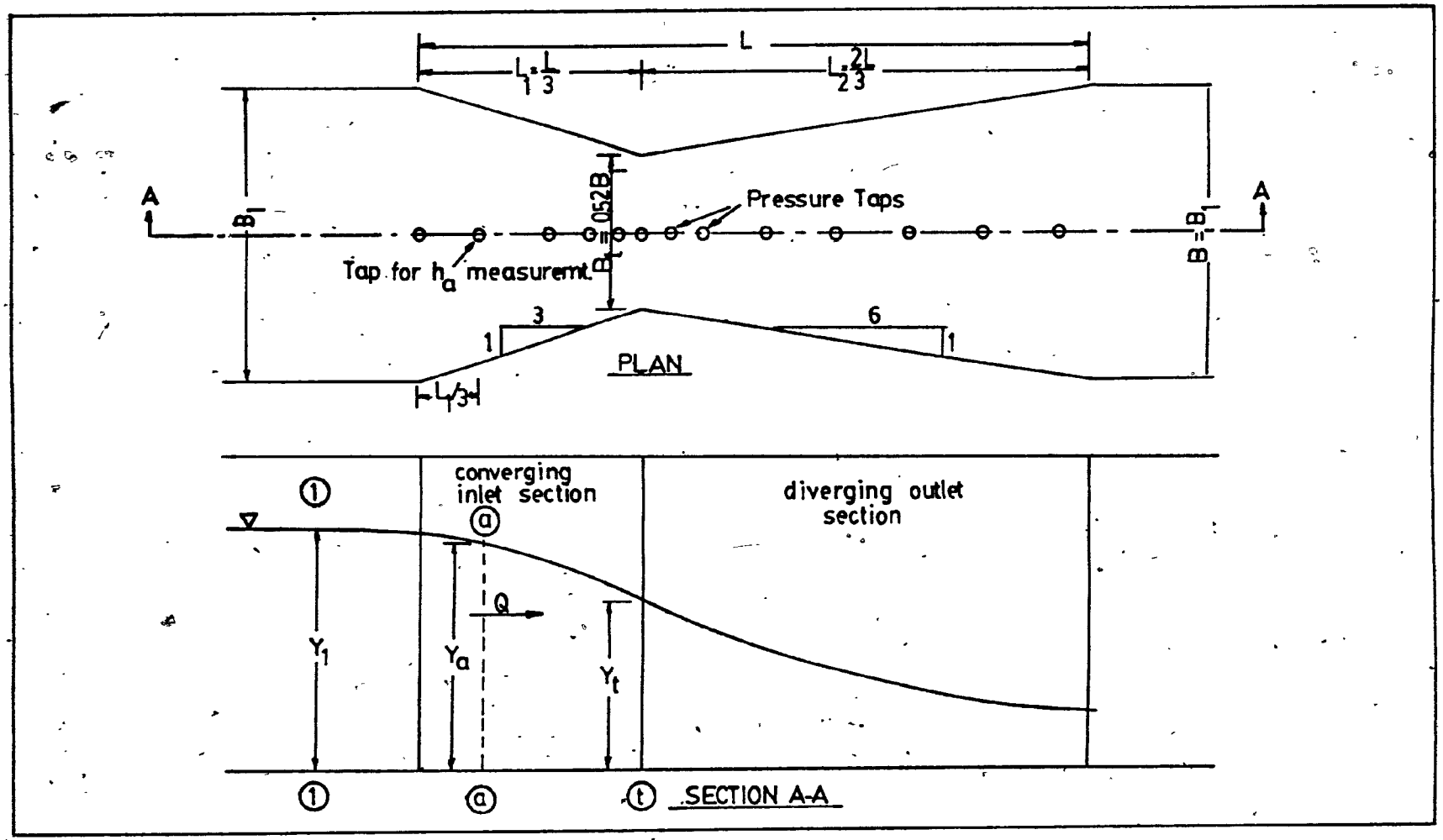

FIG. 3. DEFINITION SKETCH OF THROATLESS FLUME.

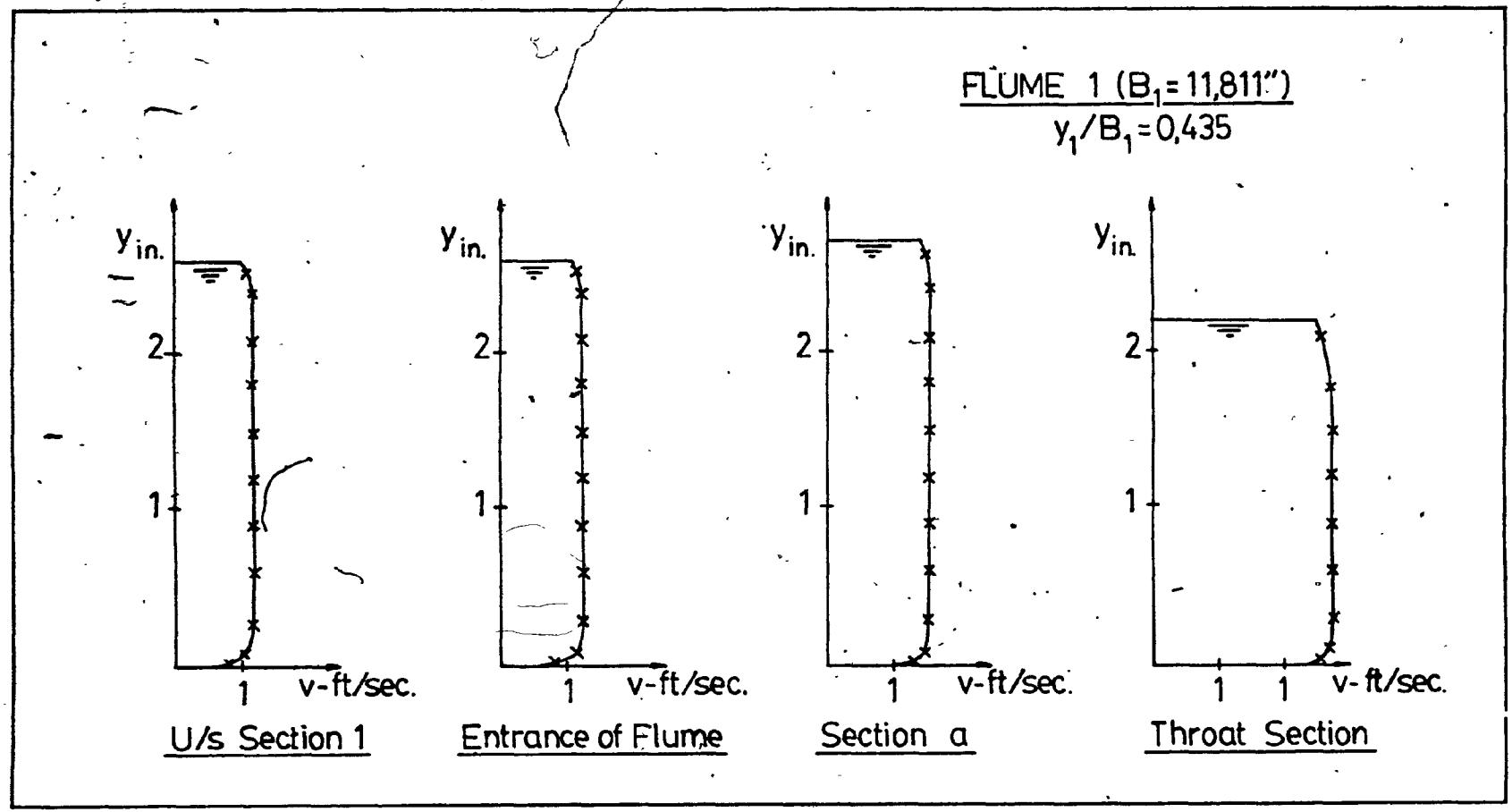

FIG. 4. VELOCITY DISTRIBUTION IN CONVERGING REACH OF FLUME.

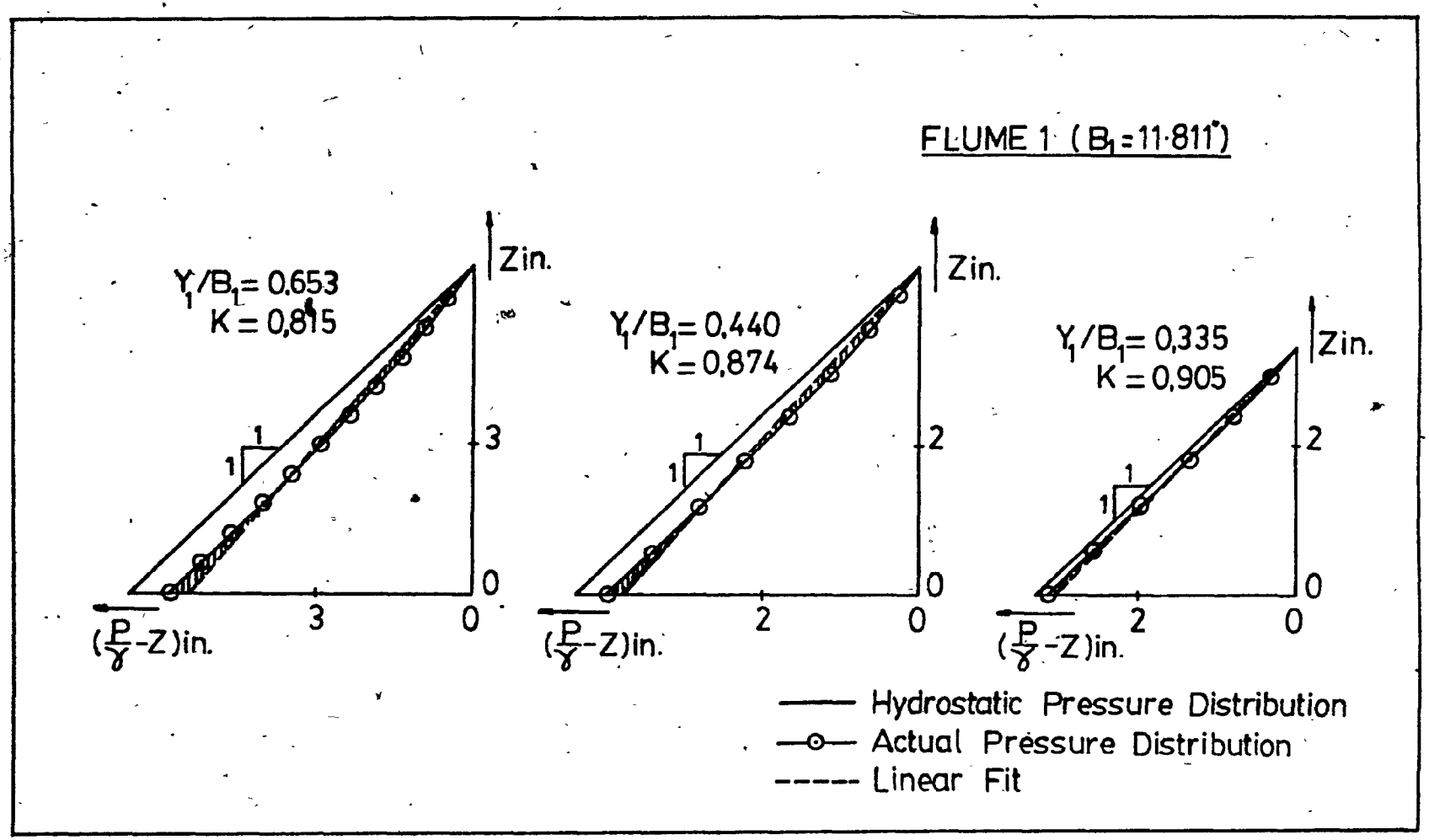

FIG. 5. PRESSURE DISTRIBUTION AT THROAT.

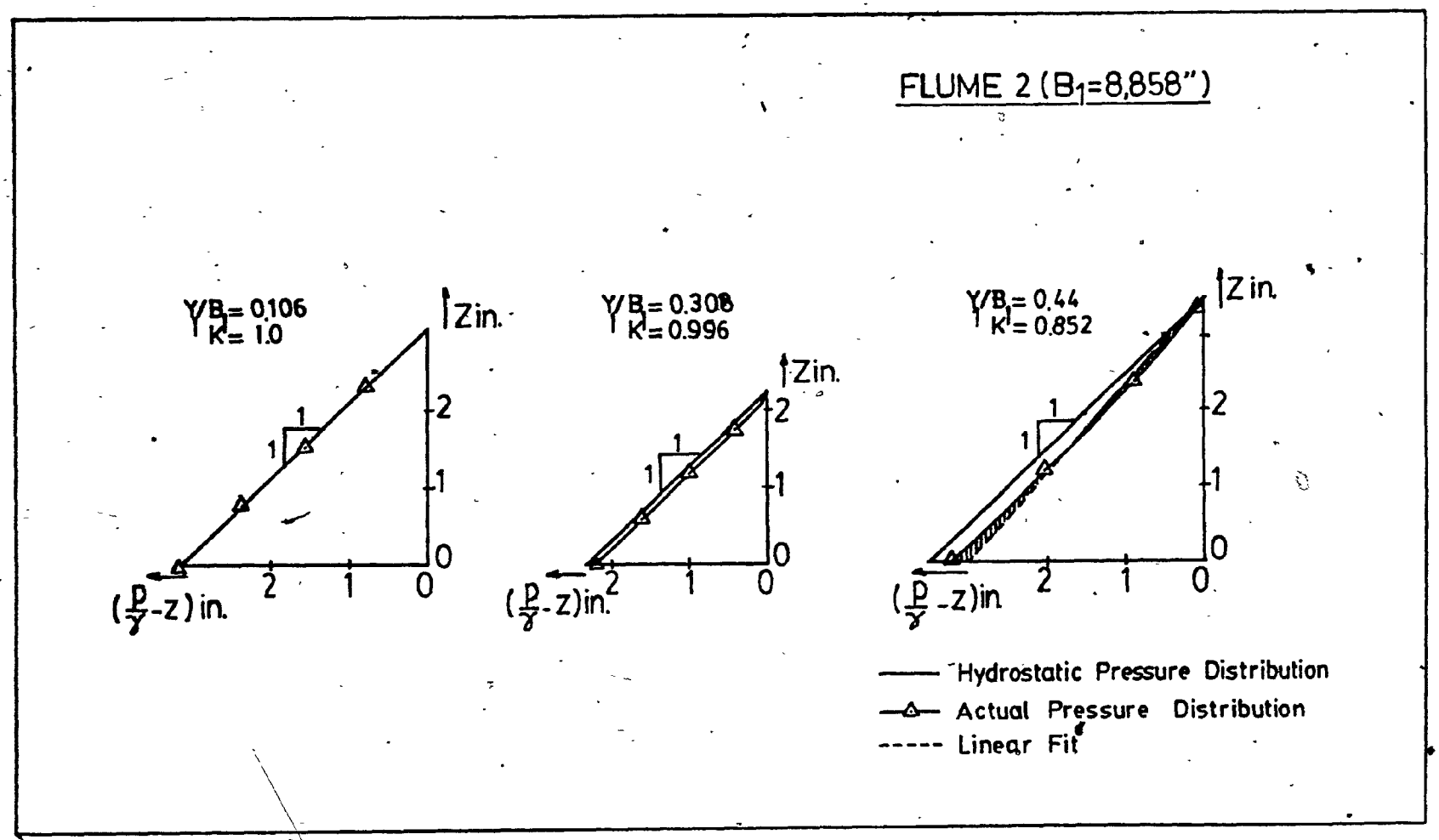

FIG. 5 (CONTINUED). PRESSURE DISTRIBUTION AT THROAT.

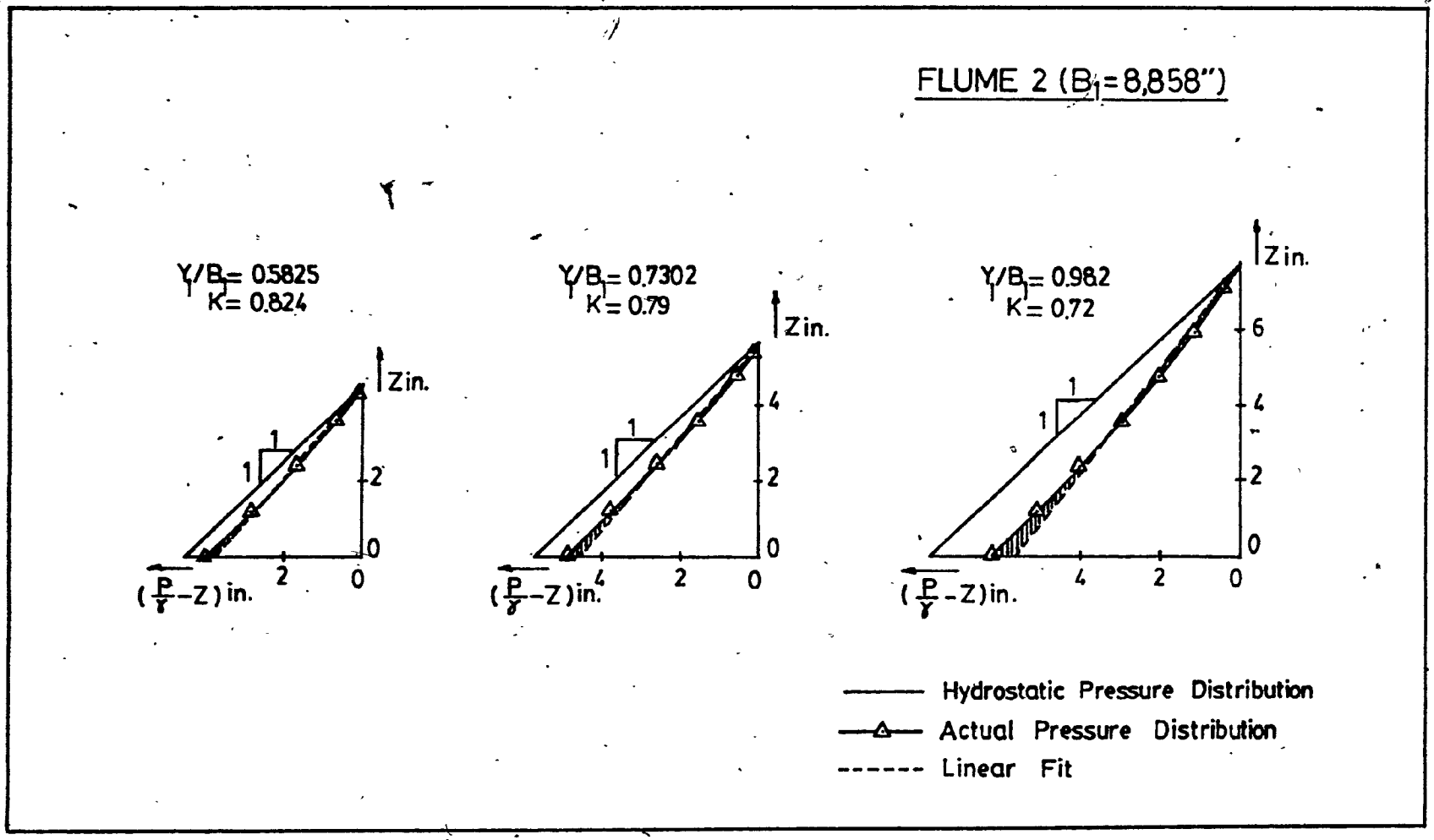

FIG. 5 (CONTINUED). PRESSURE DISTRIBUTION AT THROAT.

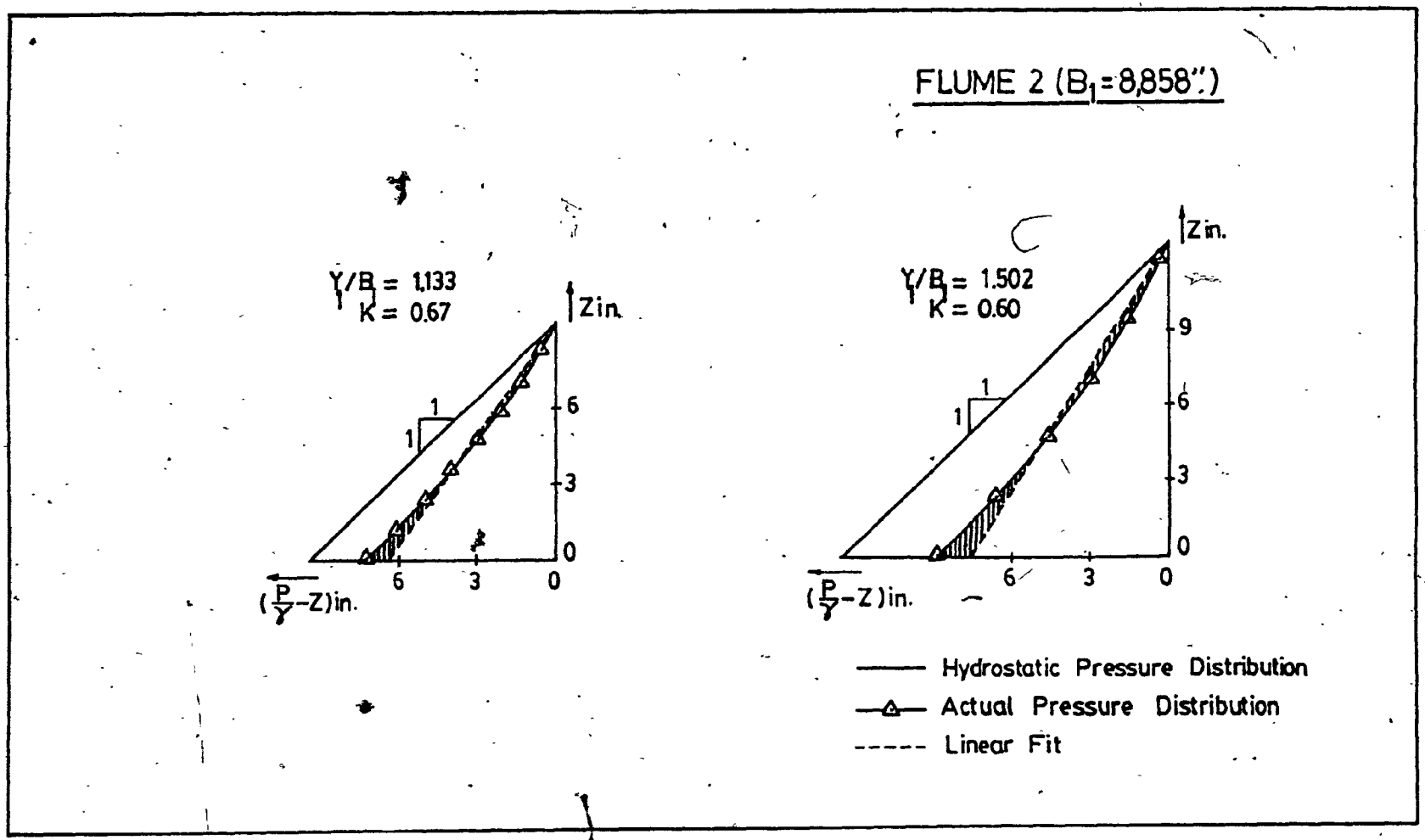

FIG. 5 (CONTINUED). PRESSURE DISTRIBUTION AT THROAT.

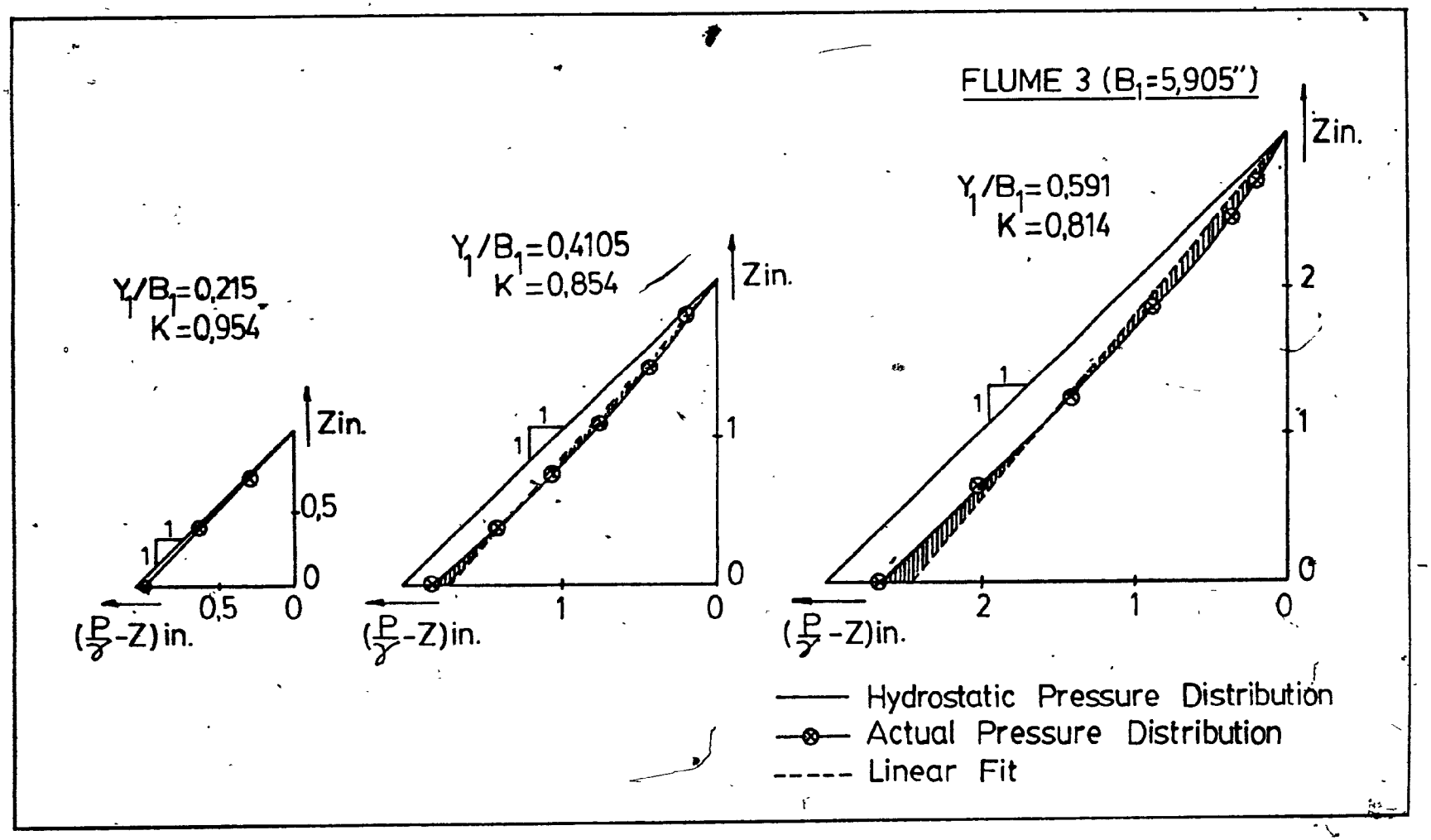

FIG. 5 (CONTINUED). PRESSURE DISTRIBUTION AT THROAT.

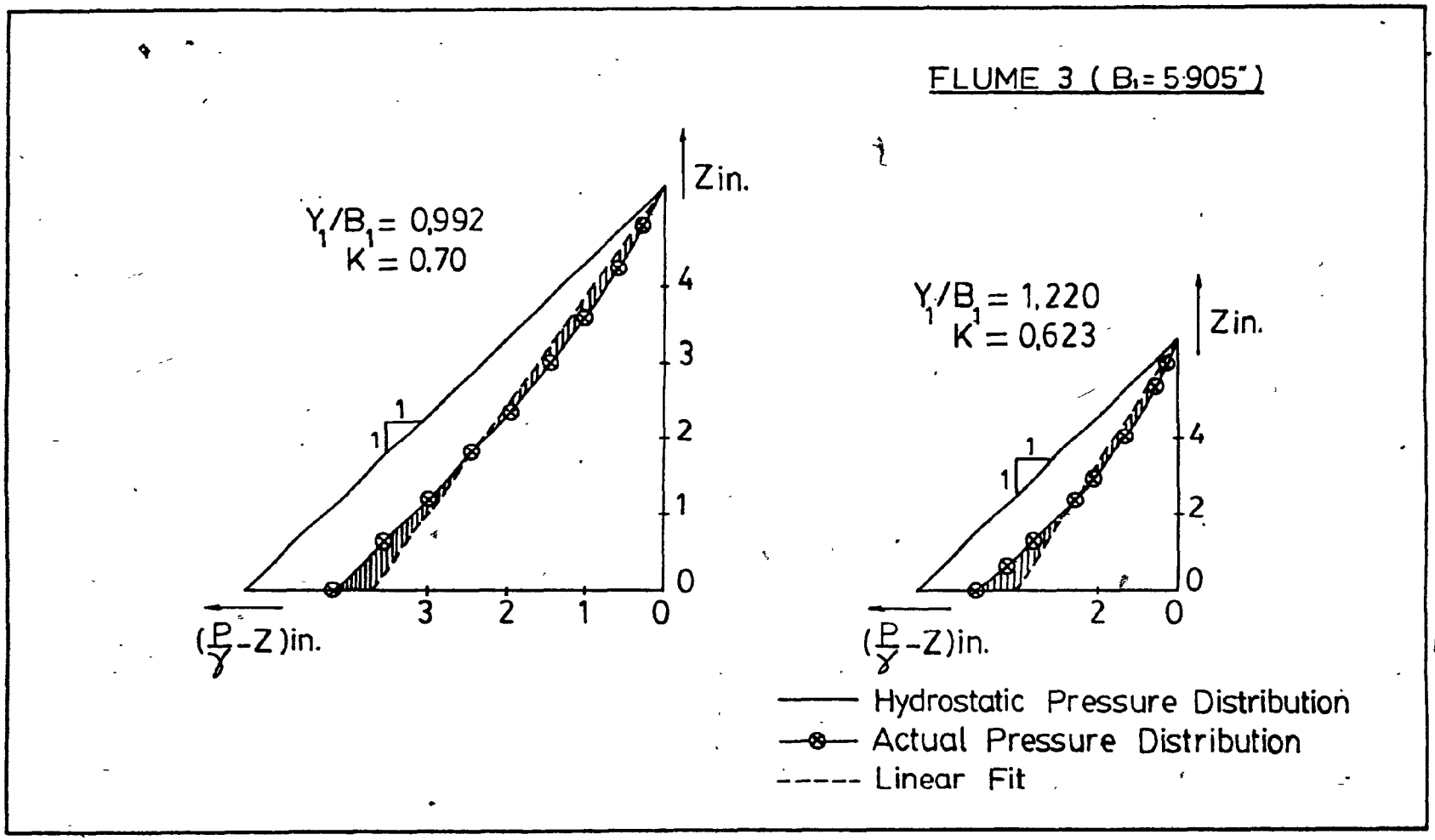

FIG. 5 (CONTINUED). PRESSURE DISTRIBUTION AT THROAT.

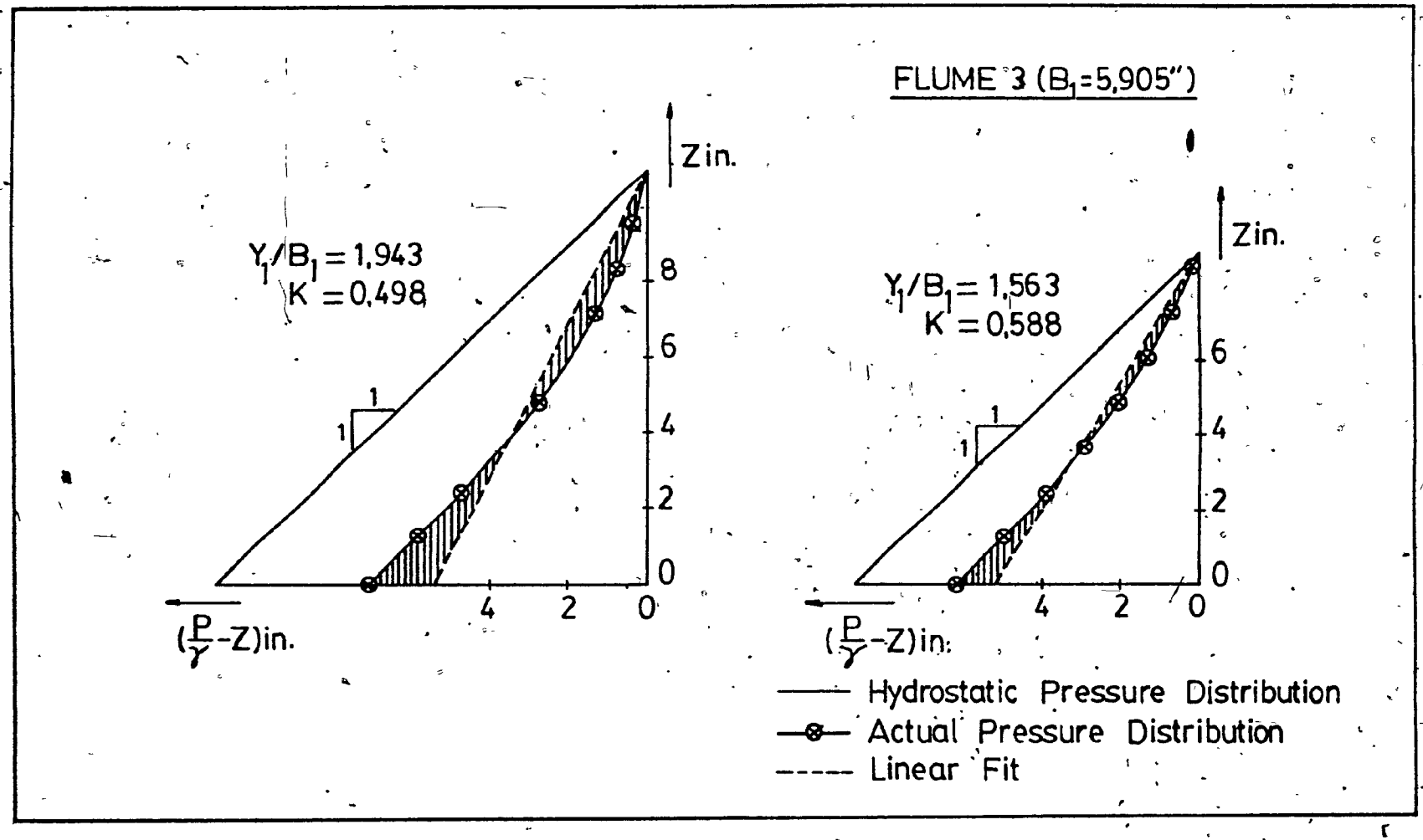

FIG. 5 (CONTINUED). PRESSURE DISTRIBUTION AT THROAT.

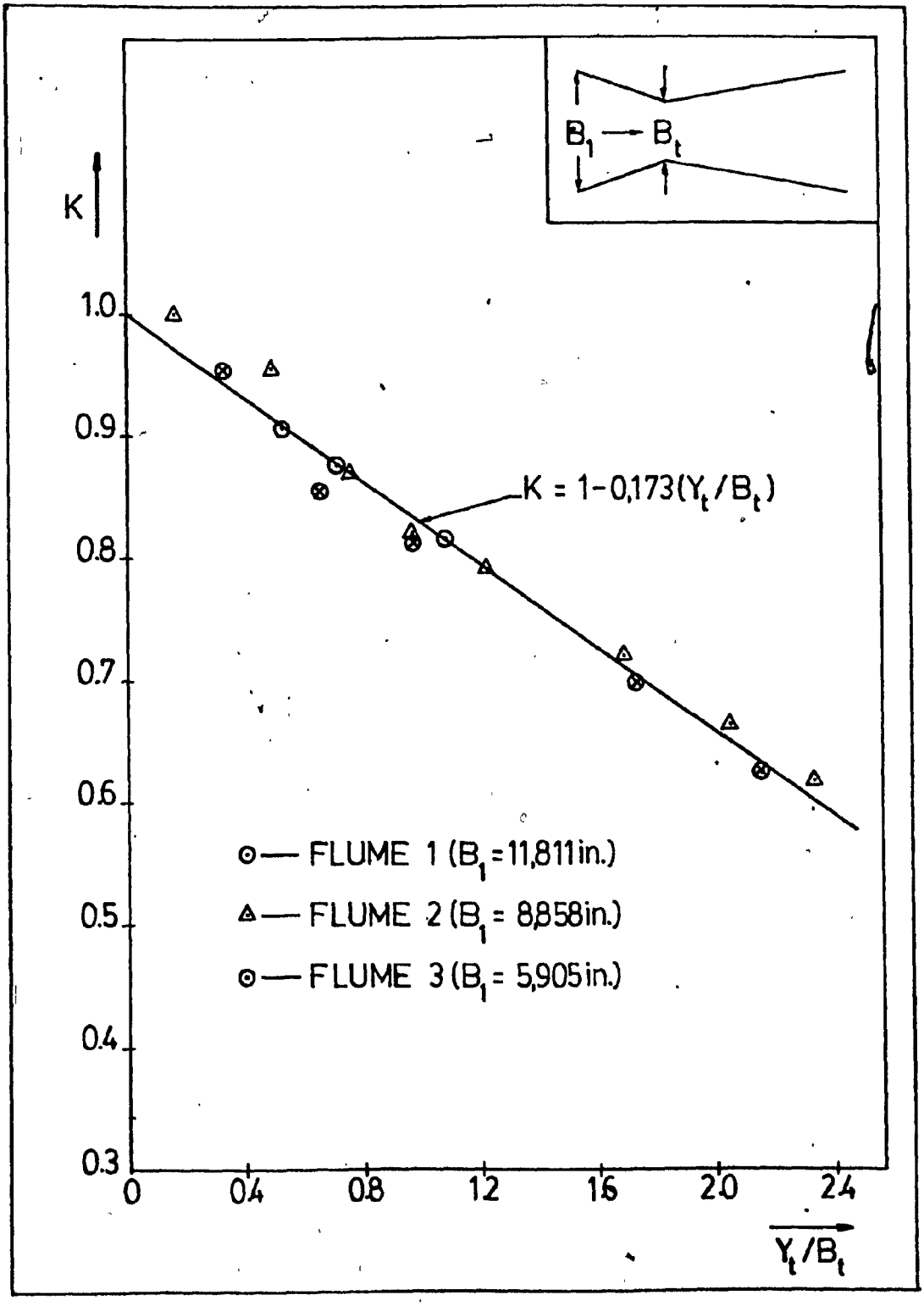

FIG. 6. VARIATION OF K WITH y_t/B_t .

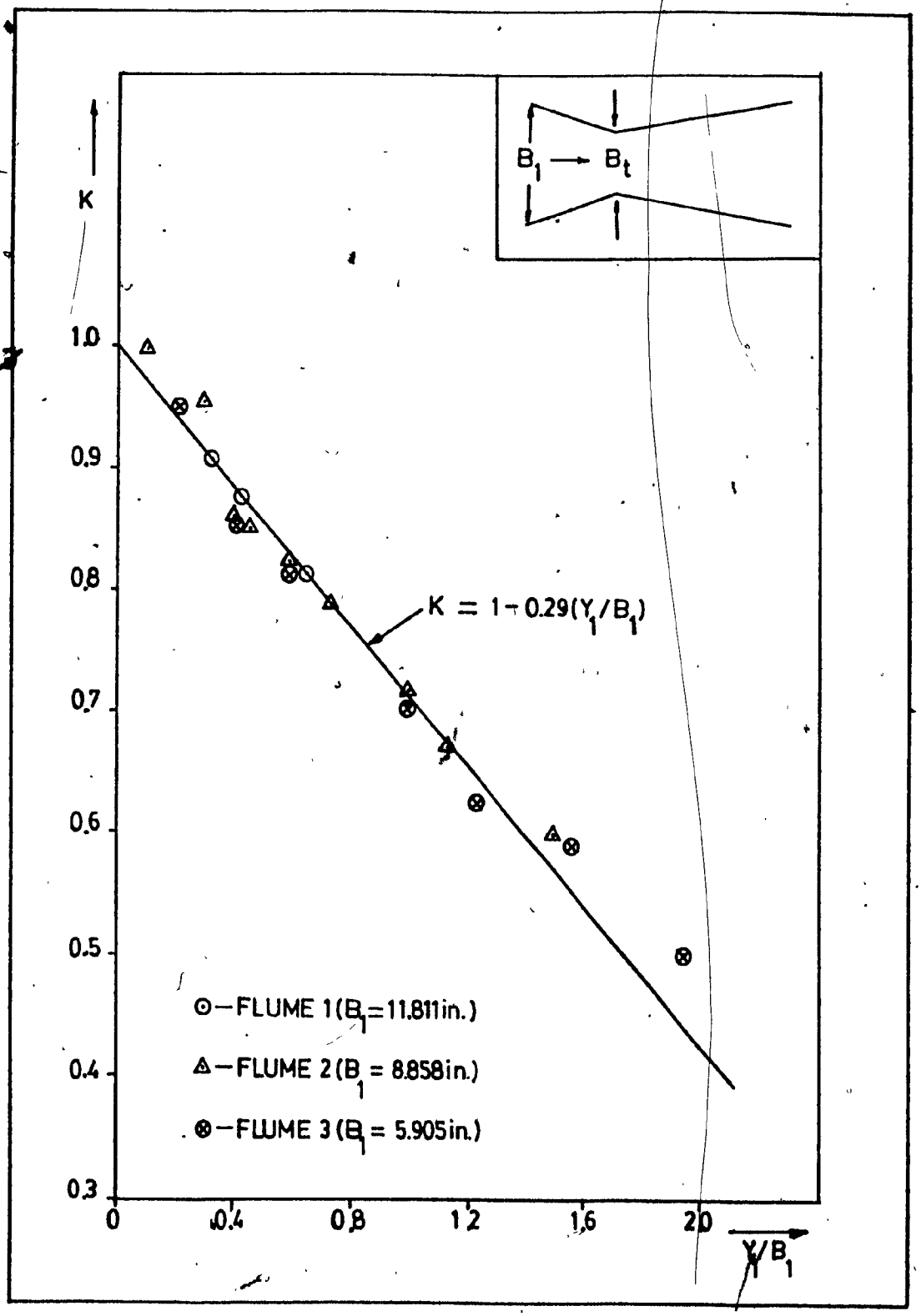

FIG. 7. VARIATION OF K WITH y_1/B_1.

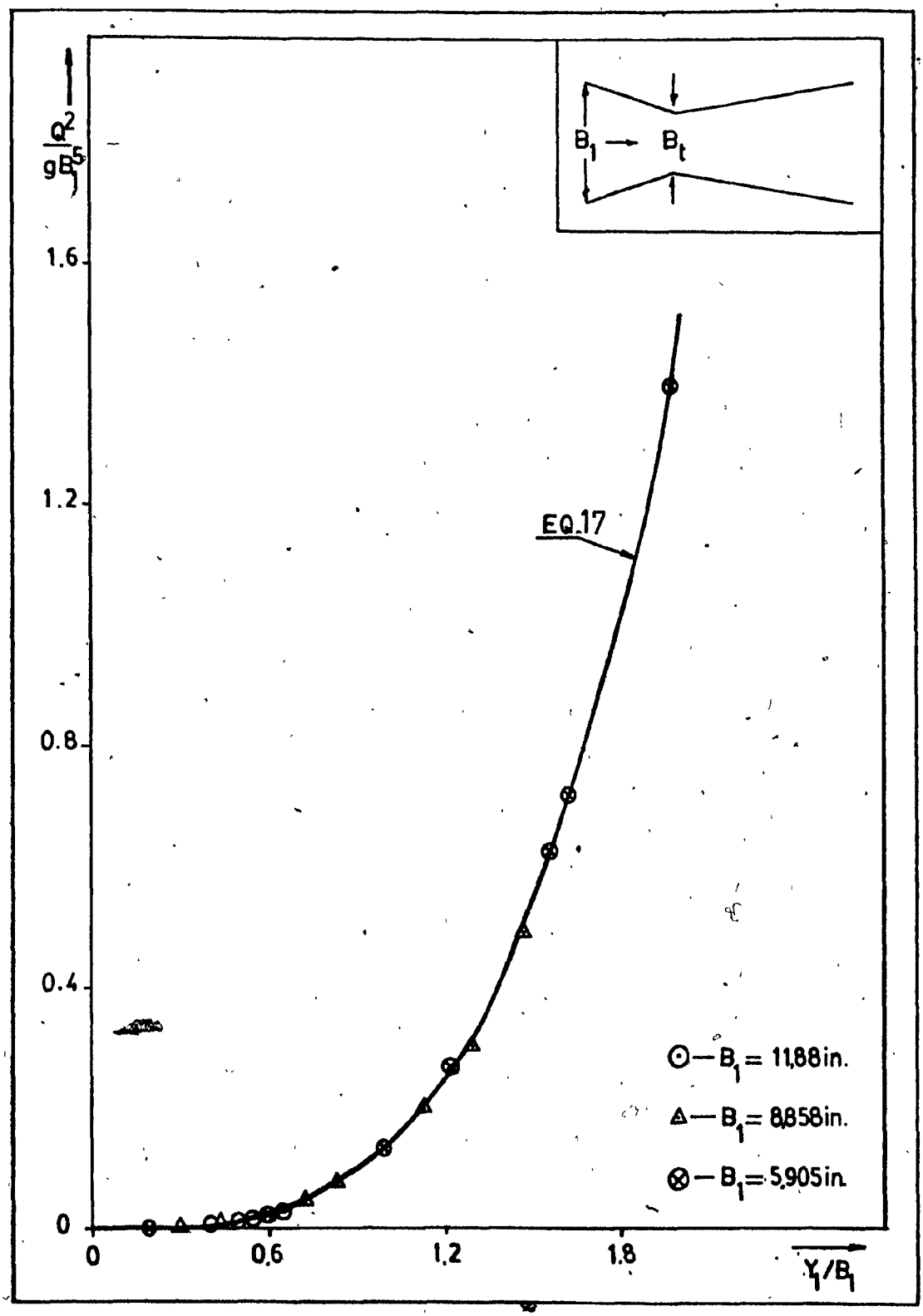

FIG. 8. VARIATION OF $Q^2/g\,B_1^5$ WITH y_1/B_1.

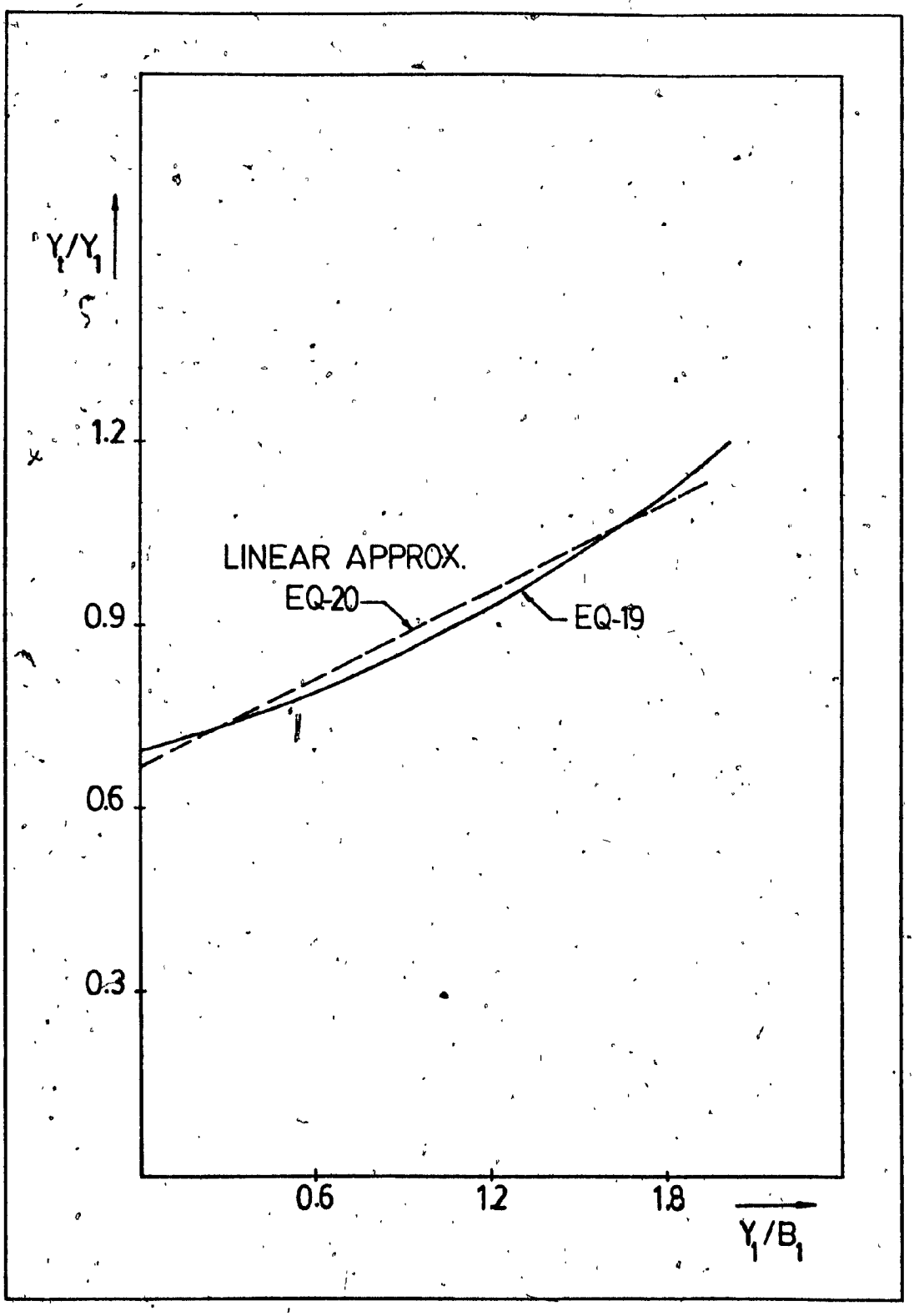

FIG. 9: VARIATION OF y_t/B_1 WITH y_1/B_1

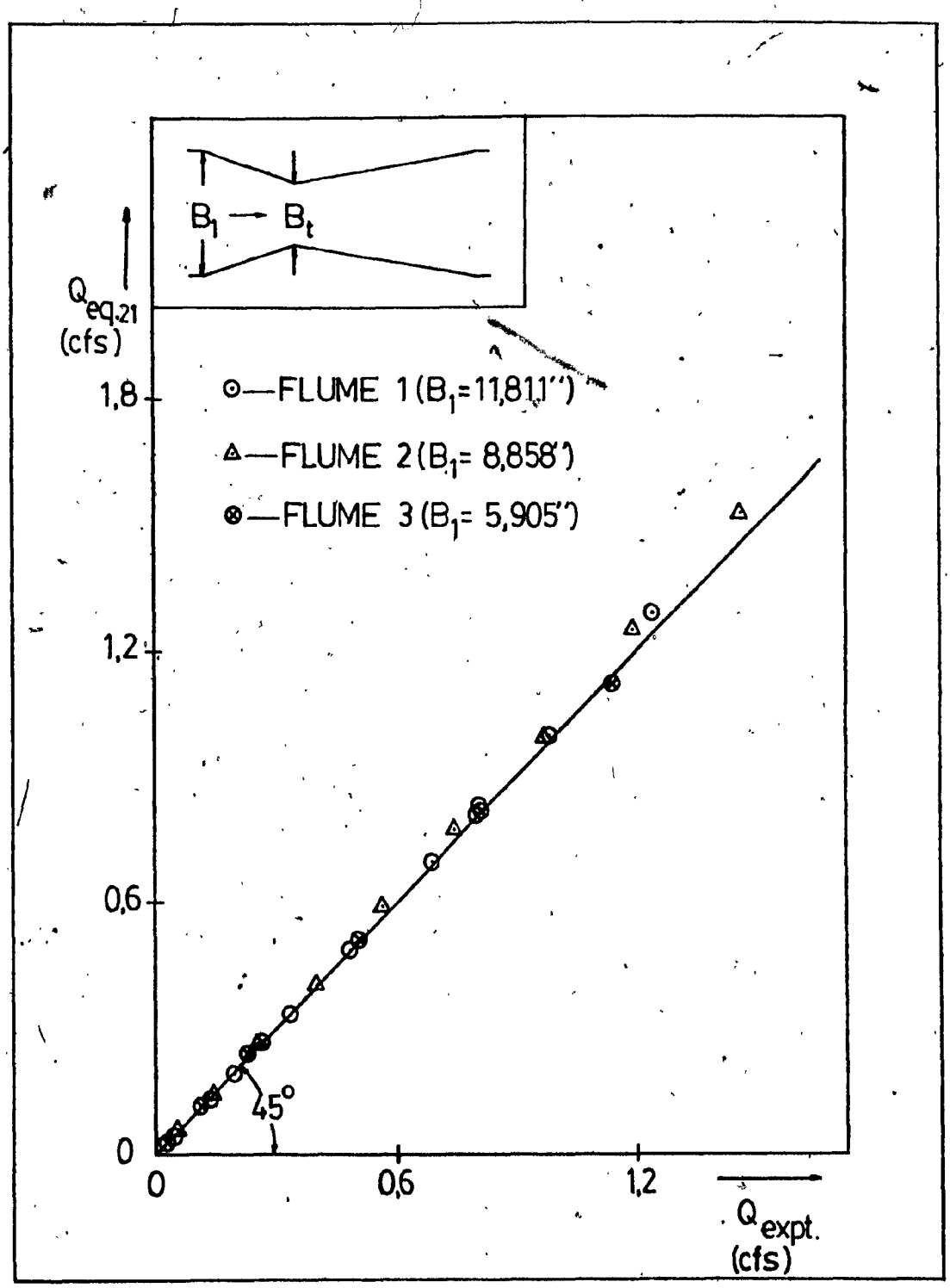

FIG. 10. VARIATION OF $Q_{exp.}$ WITH $Q_{comp.}$ (EQ. 21).

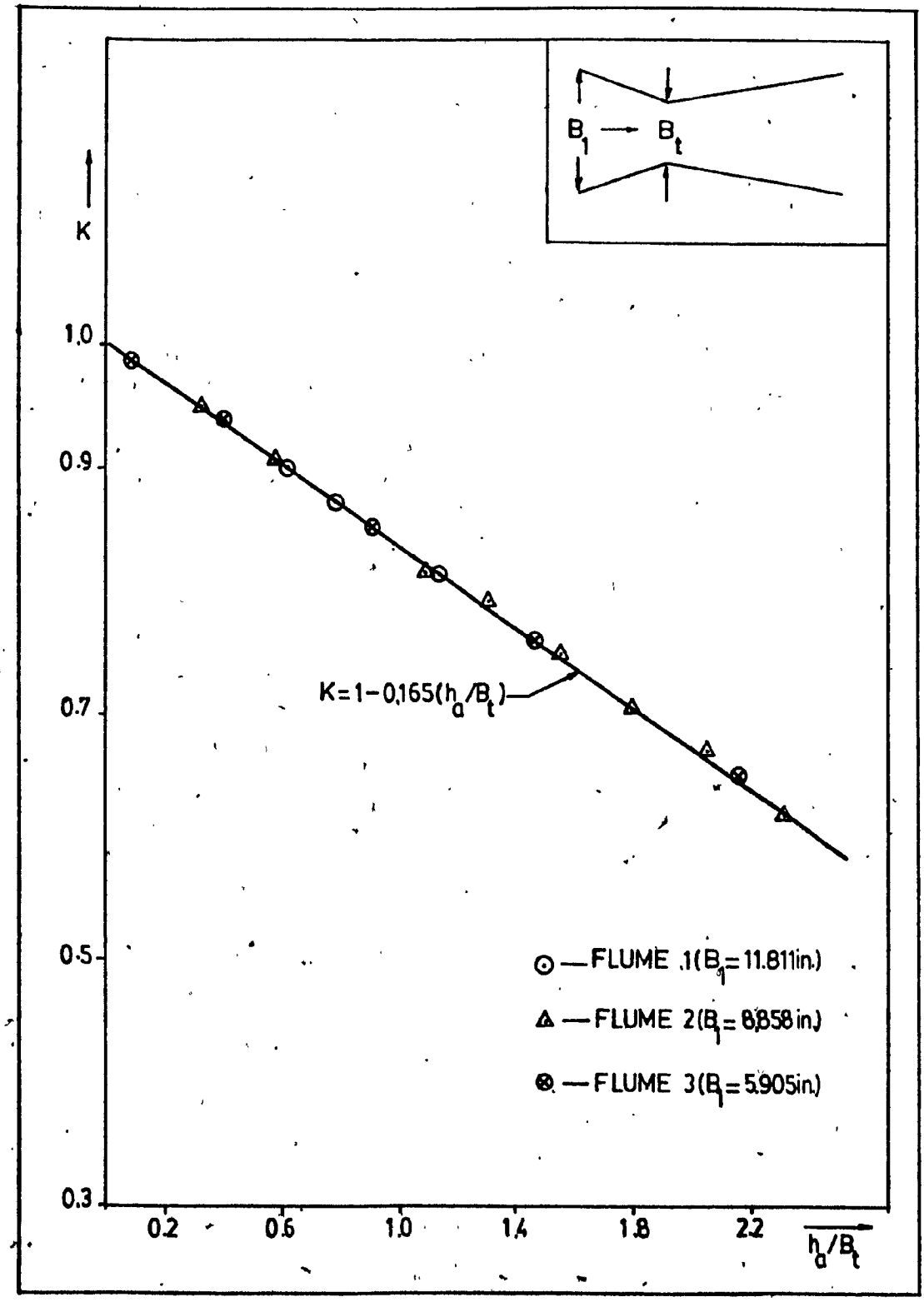

FIG. 11. VARIATION OF K WITH h_a/B_t .

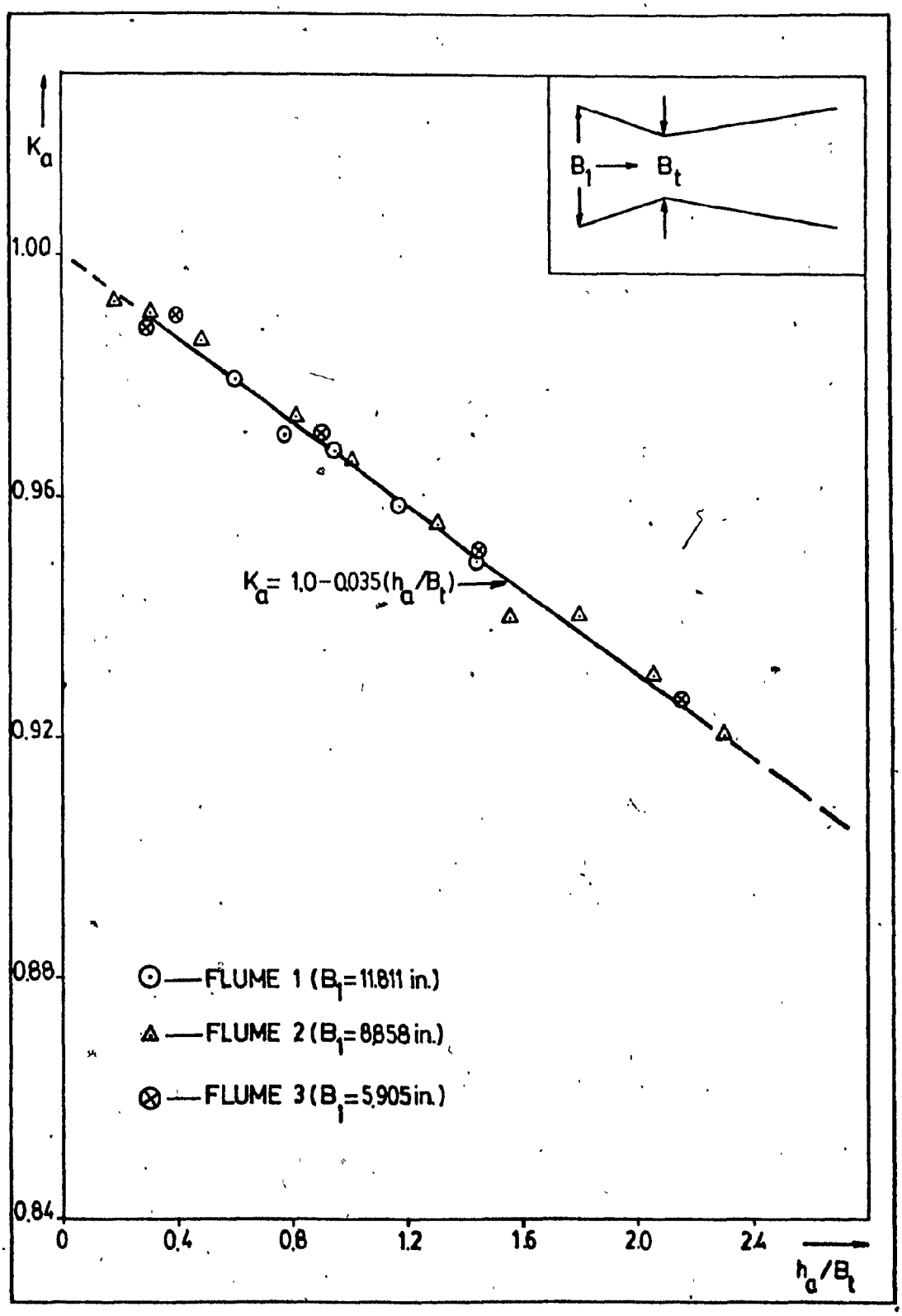

FIG. 12. VARIATION OF K_a WITH h_a/B_t.

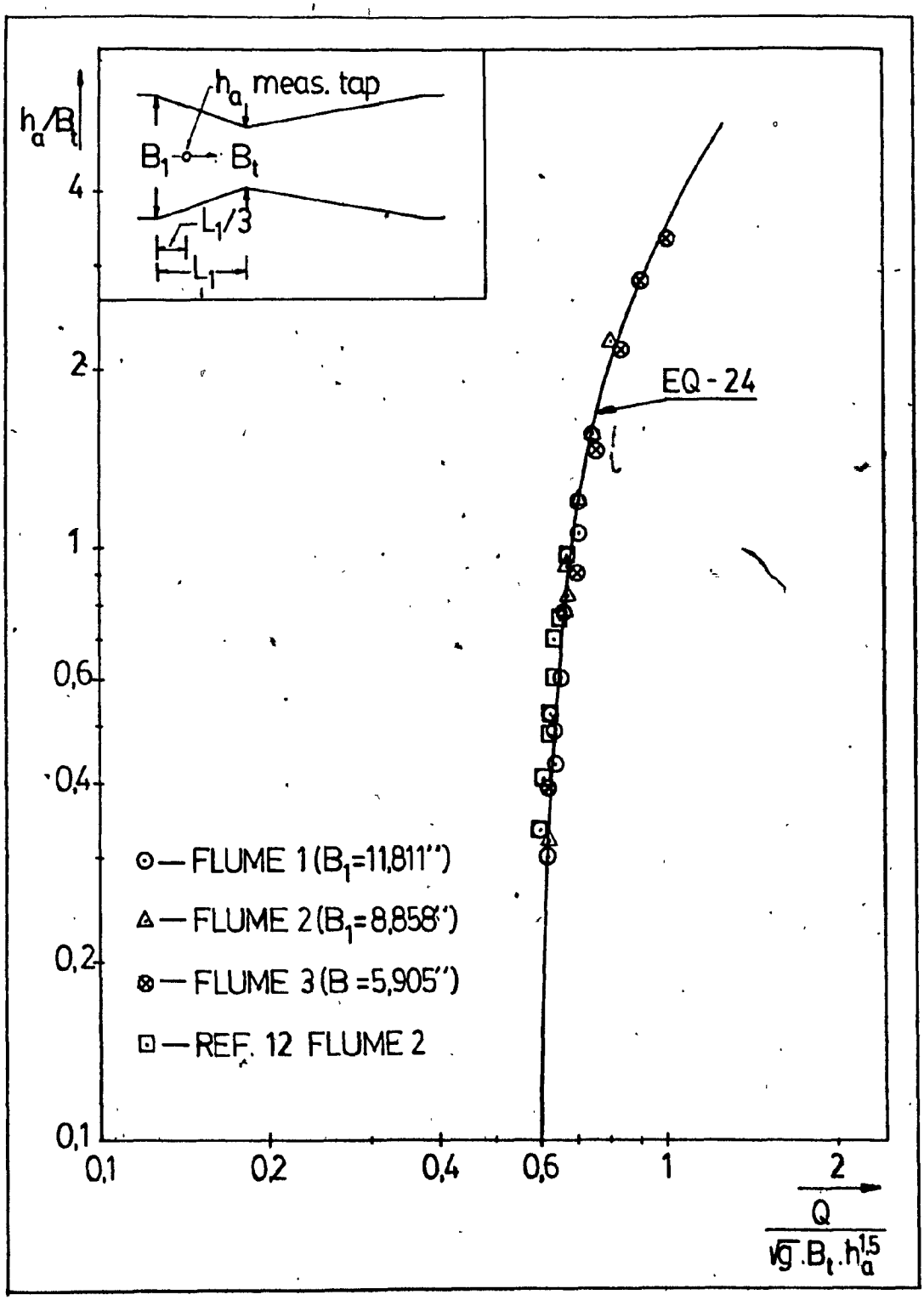

FIG. 13. VARIATION OF h_a/B_t WITH $Q/\sqrt{g}\ B_t\ h_a^{1.5}$.

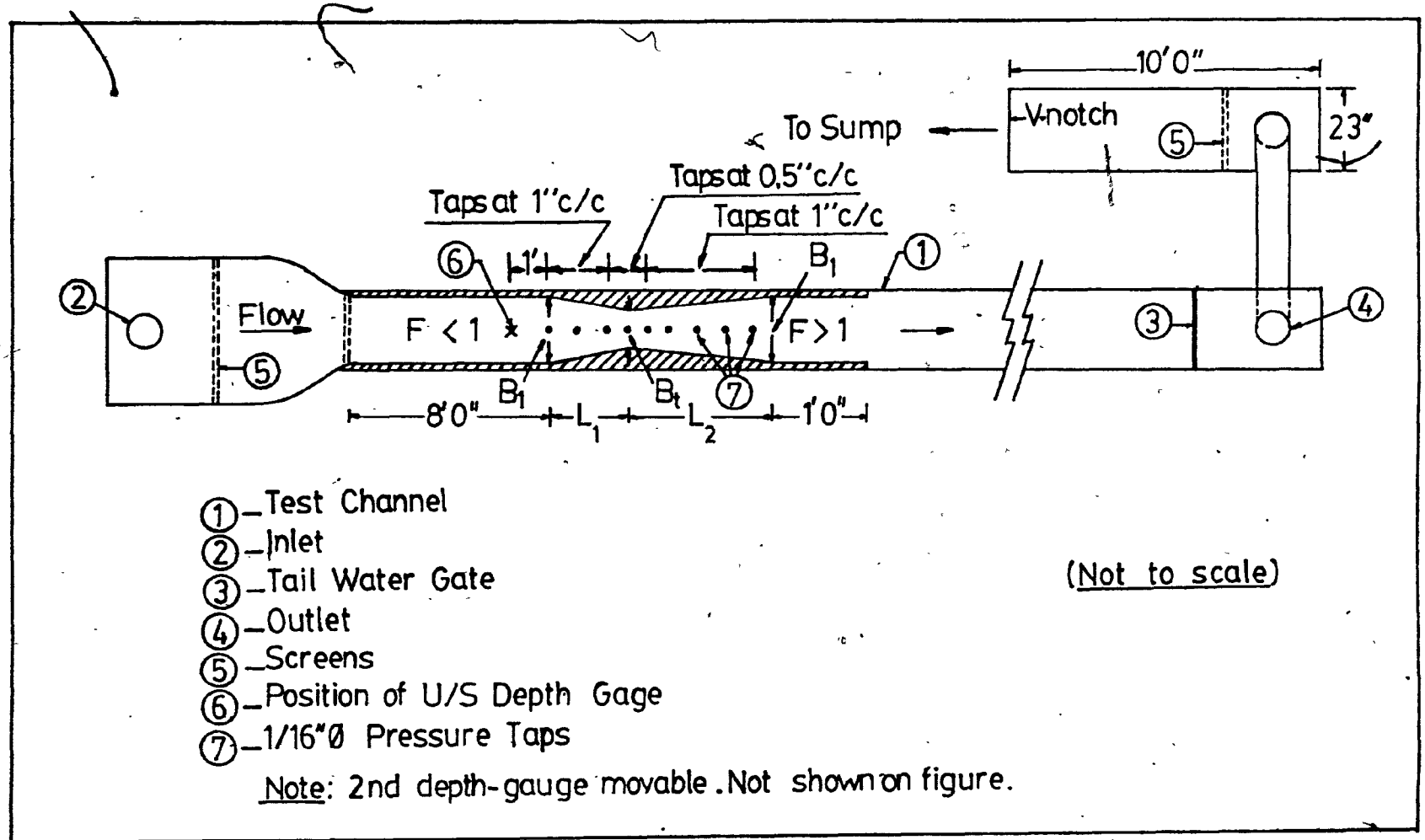

FIG. 14. SCHEMATIC LAYOUT PLAN OF EXPERIMENTAL SET-UP.

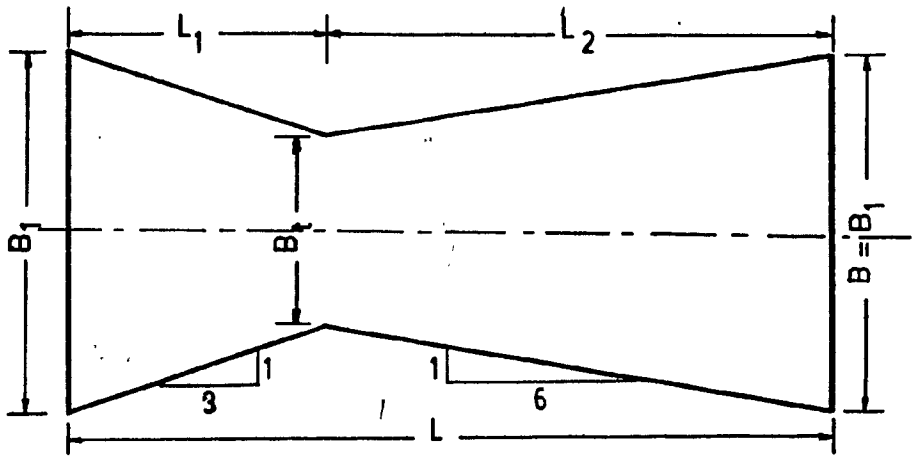

FLUME	B_1 inches	L_1 inches	L_2 inches	L inches	B_1 inches
1	6.142	8.504	17.008	25.512	11.811
2	4.606	6.378	12.756	19.134	8.858
3	3.071	4.252	8.504	12.756	5.905

FIG. 15. DETAILS OF TEST FLUMES.

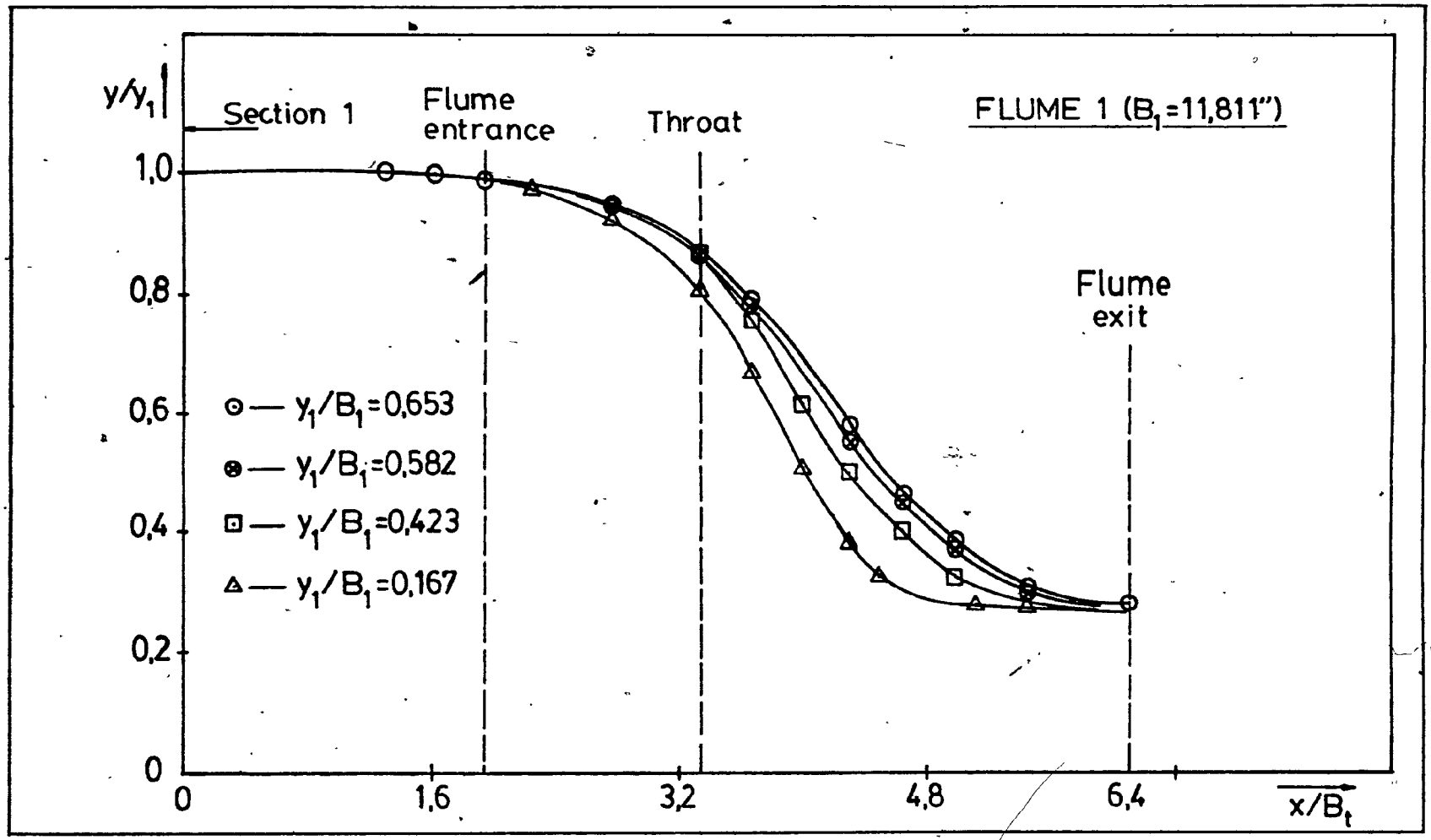

FIG. 16. WATER SURFACE PROFILES.

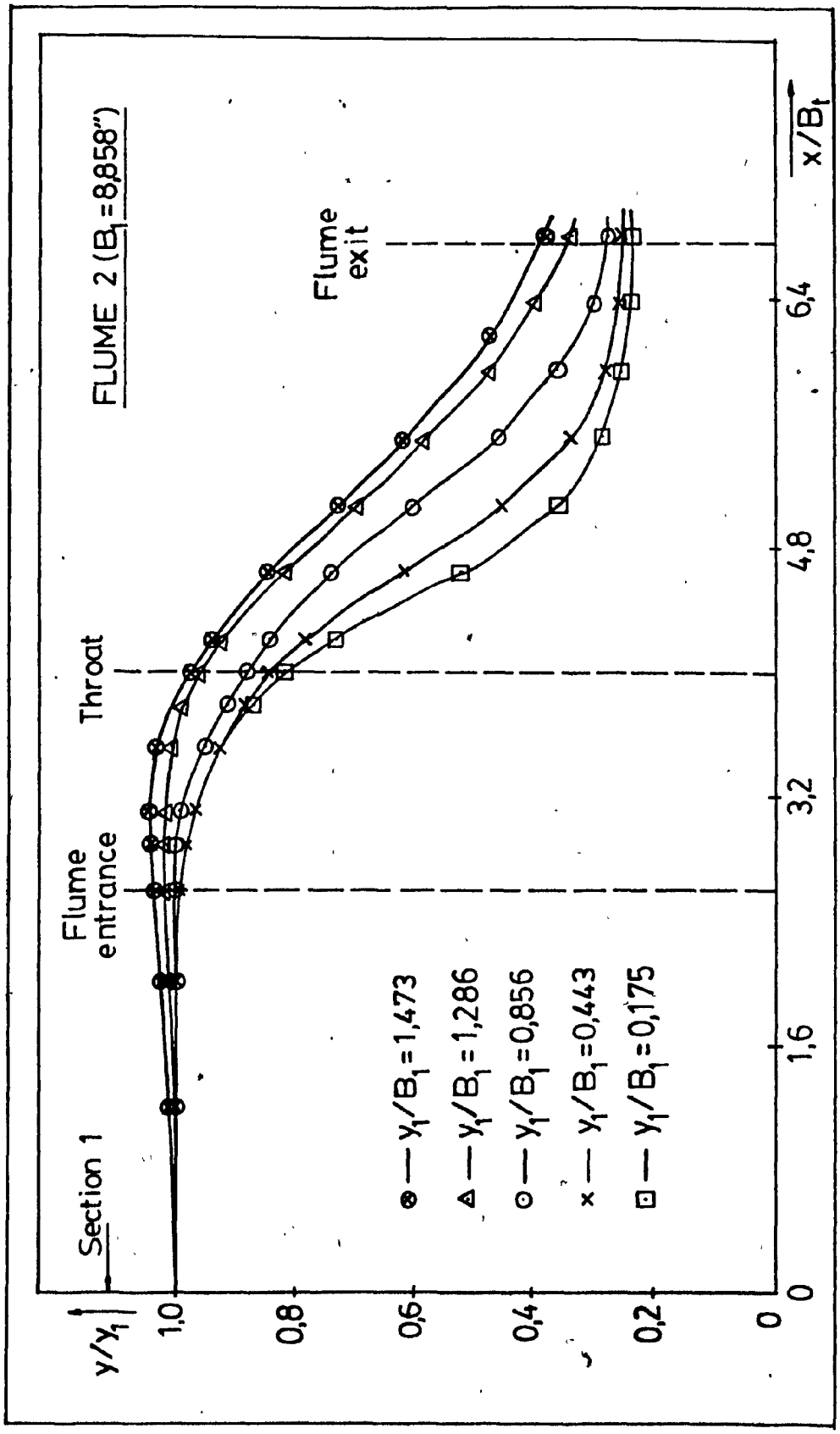

FIG. 16 (CONTINUED). WATER SURFACE PROFILES.

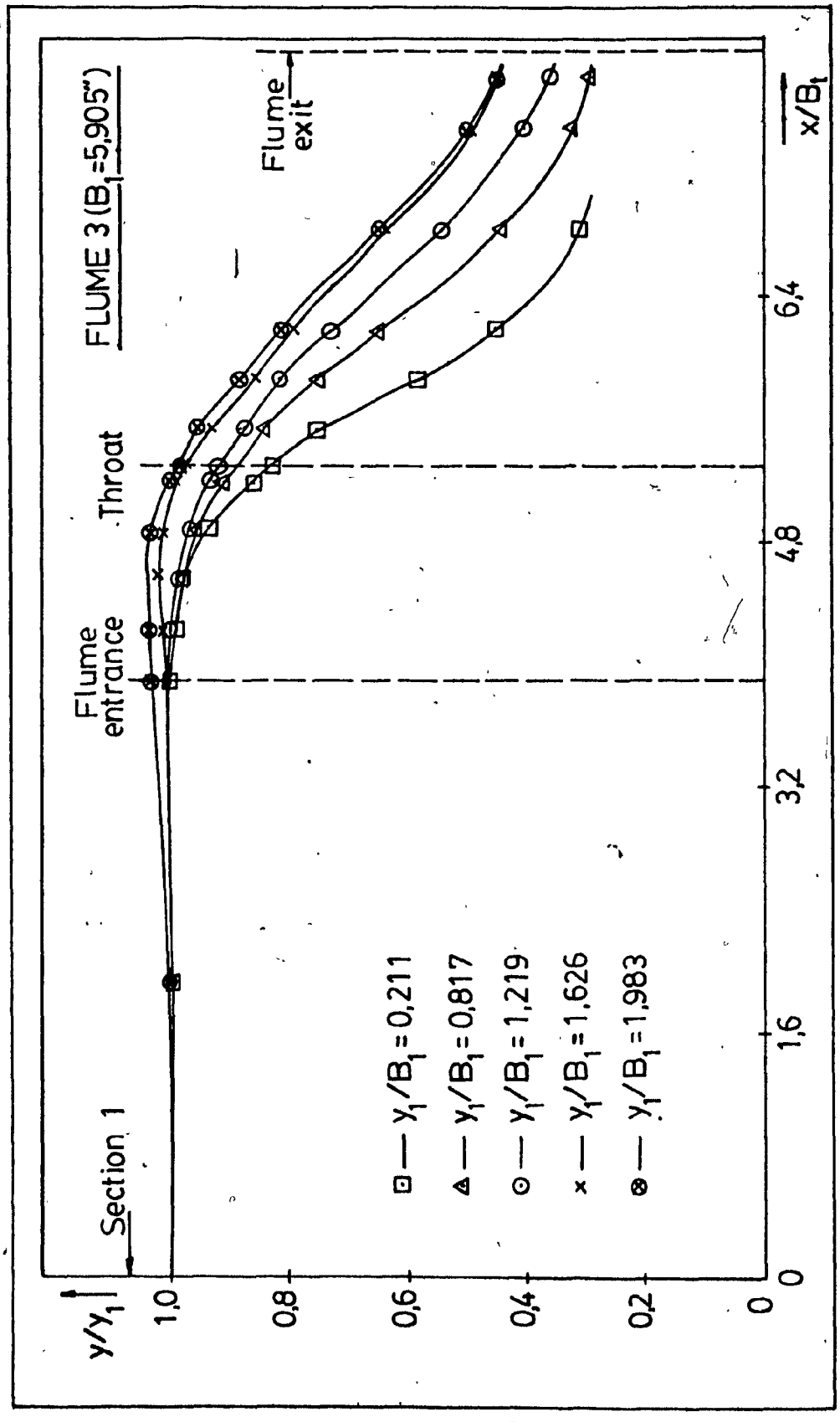

FIG. 16 (CONTINUED). WATER SURFACE PROFILES.

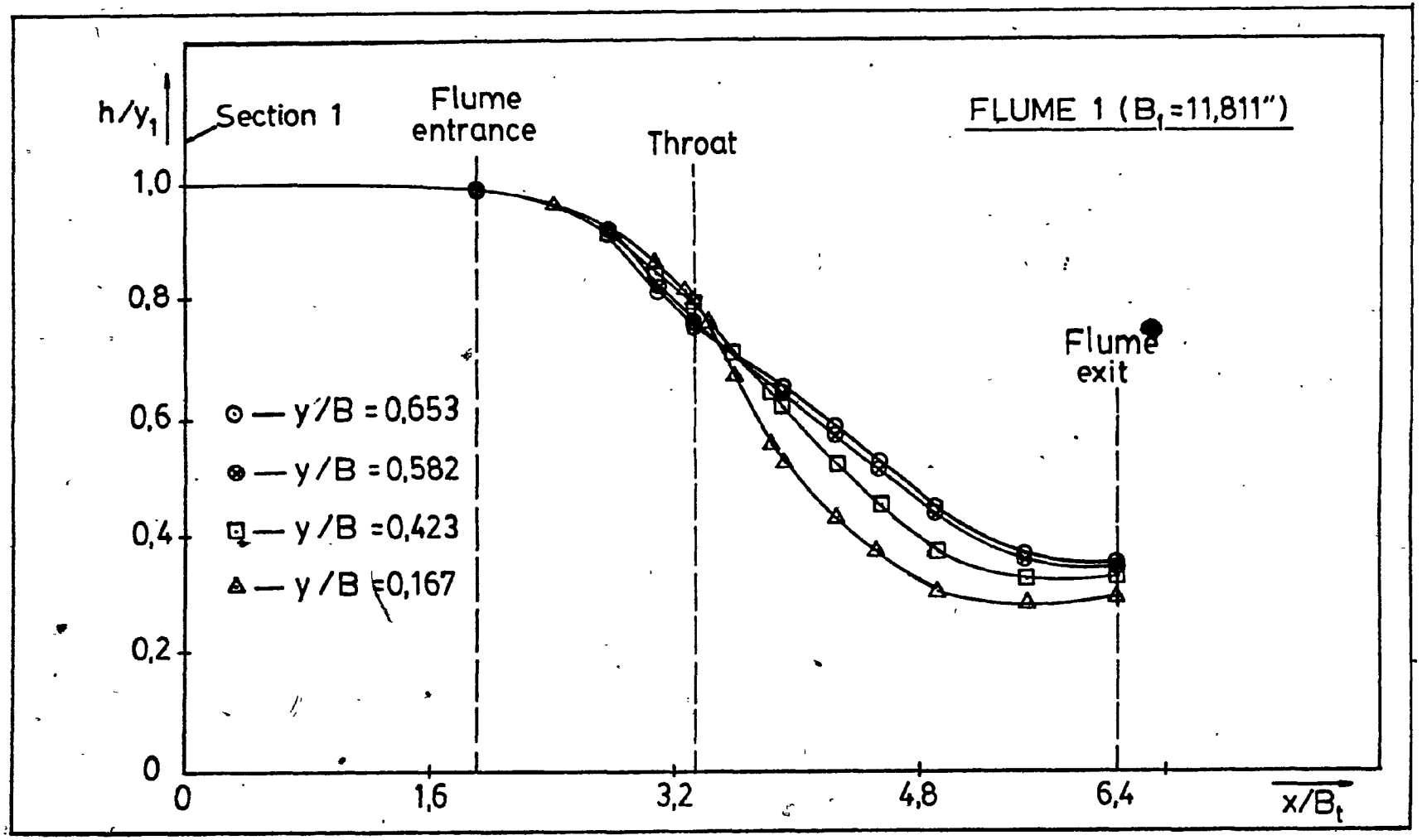

FIG. 17. FLOOR PRESSURE PROFILES.

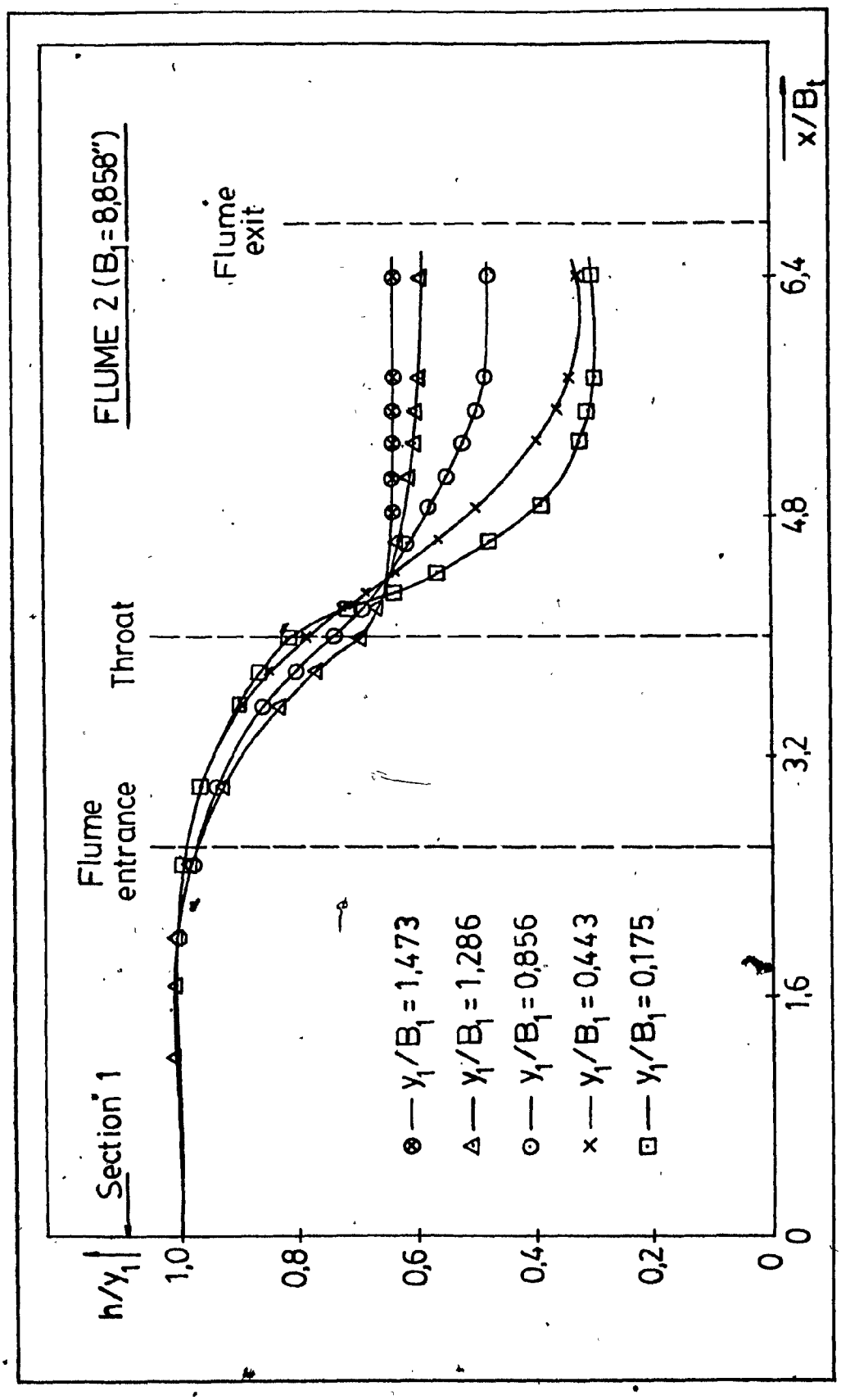

FIG. 17 (CONTINUED). FLOOR PRESSURE PROFILES.

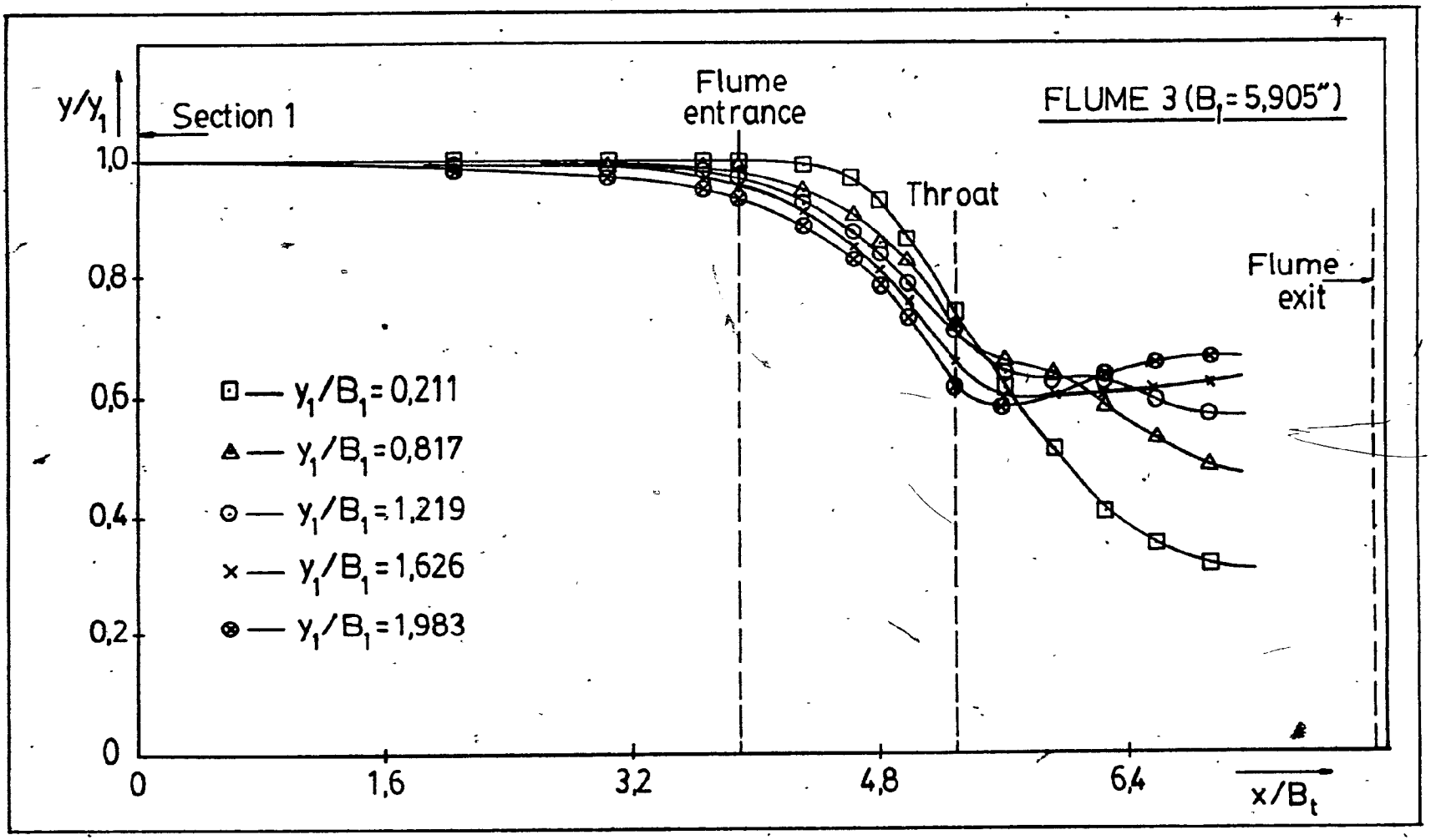

FIG. 17 (CONTINUED). FLOOR PRESSURE PROFILES.

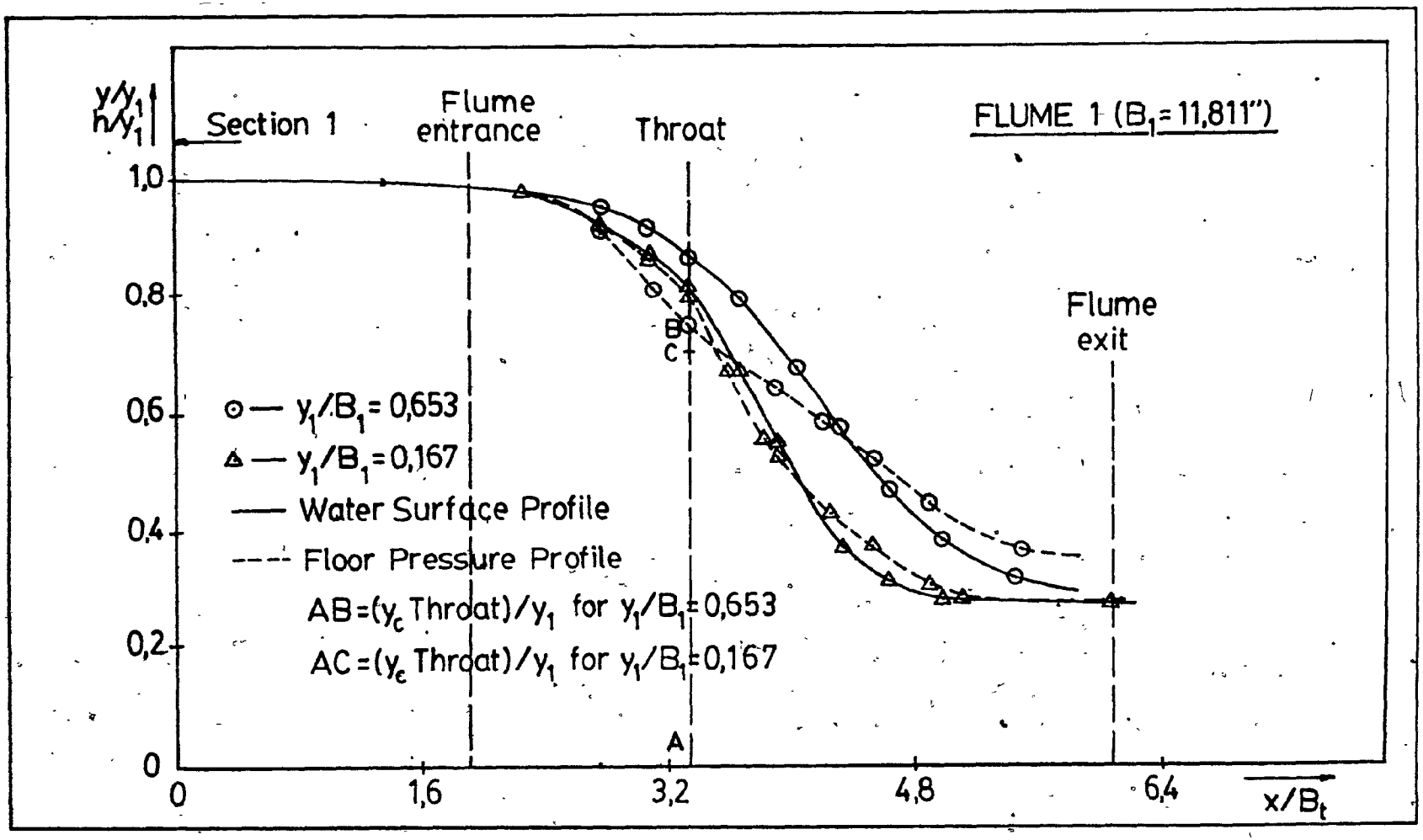

FIG. 18. TYPICAL FLOOR PRESSURE AND SURFACE PROFILES.

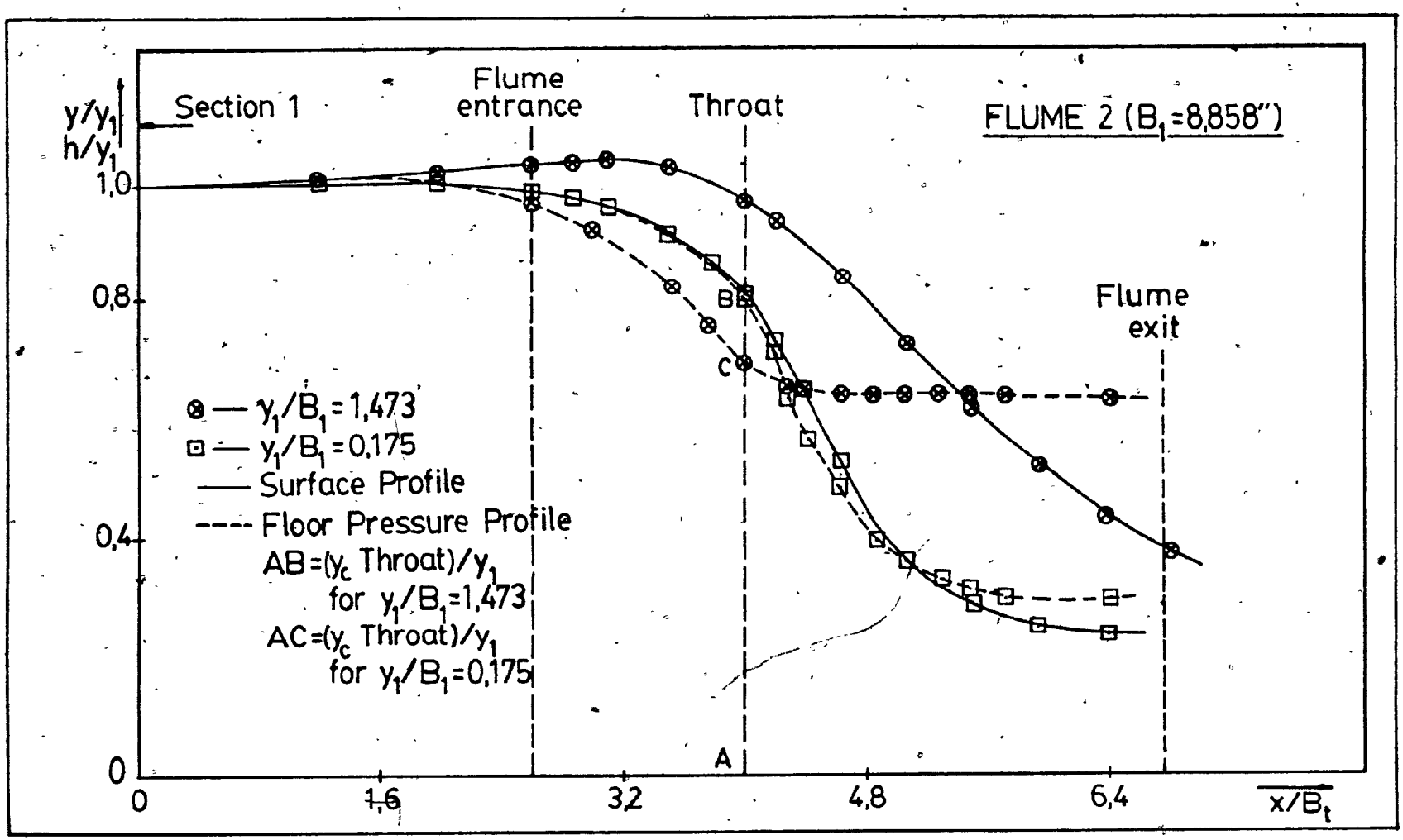

FIG. 18 (CONTINUED). TYPICAL FLOOR PRESSURE AND SURFACE PROFILES.

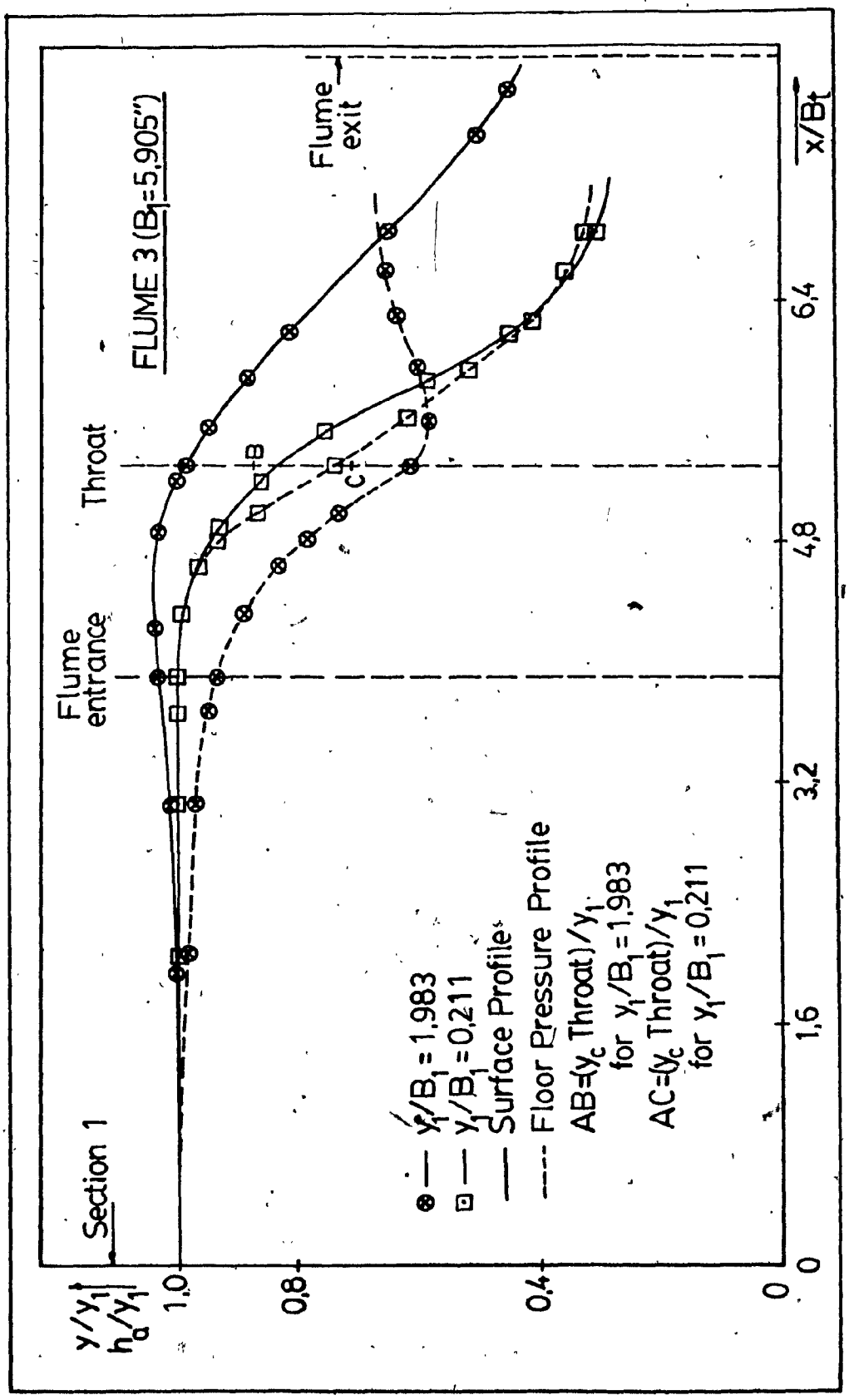

FIG. 18 (CONTINUED). TYPICAL FLOOR PRESSURE AND SURFACE PROFILES.

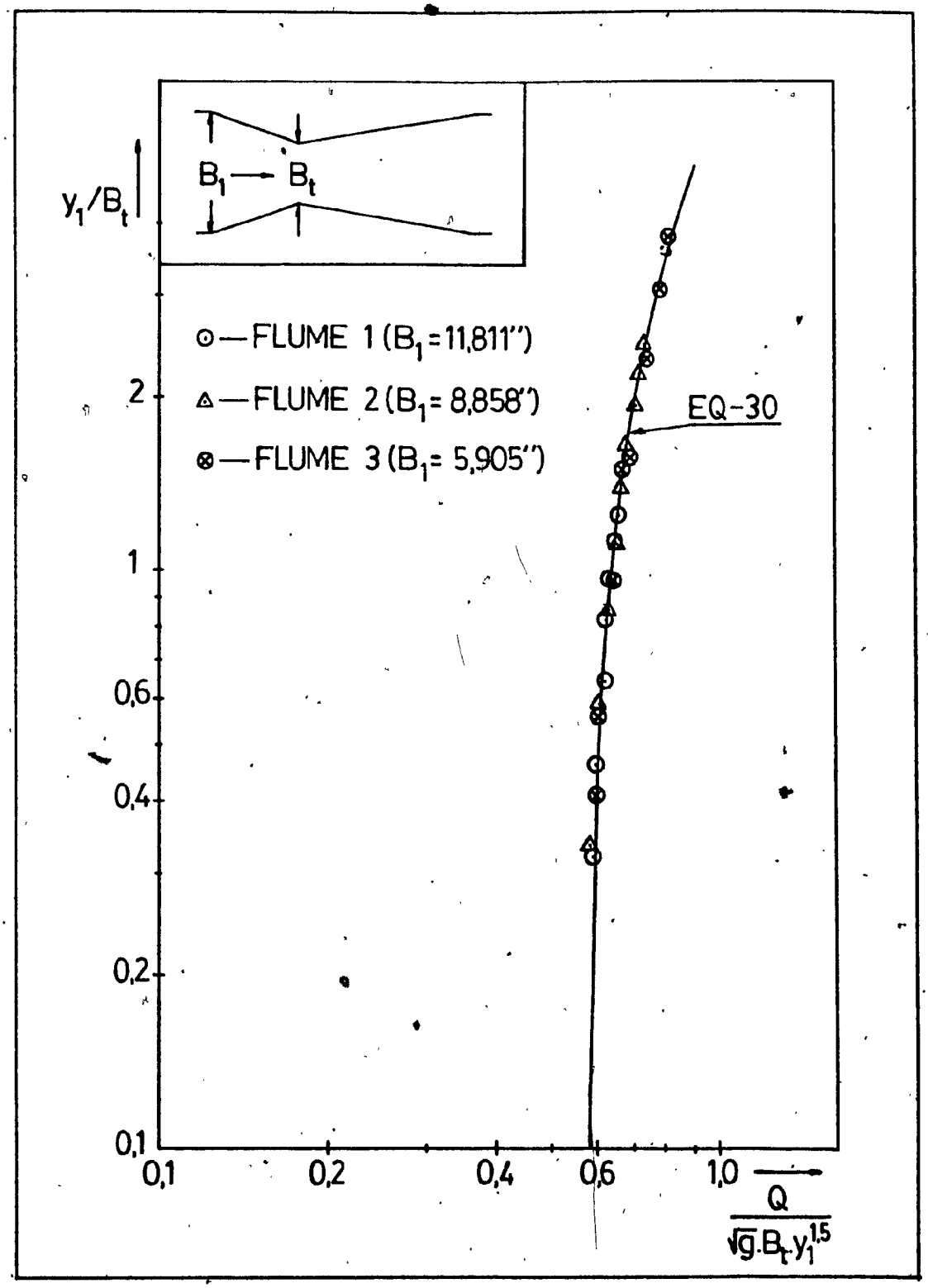

FIG. 19. VARIATION OF y_1/B_t WITH $Q/\sqrt{g}\, B_t\, y_1^{1.5}$.

APPENDIX III

TABLES AND EXPERIMENTAL DATA

Table 1. Typical Critical Depth Flumes

References	Type of Flume	Relevant Features	Discharge Characteristics Developed	Remarks
Cone, V.M. (6) Engel, F.V.A. (7) Ackers, P. et al (1)	The Venturi Flume	Rectangular and Trapezoidal shapes. Has short parallel throat; level floor.	Rating tables developed. Engel later developed discharge equations with discharge coefficients determined experimentally.	Non-geometrically similar models tested.
Parshall, R.L. (17, 18)	Parshall Flume	Floor is level in converging section, downward sloping in parallel throat, upward sloping in diverging section. Rectangular shapes.	Empirical equation for free discharge; Modular limit 70%; Also Rating Curves and Tables developed; High accuracy.	The flumes are not geometrically similar. Very widely used flume in irrigation (U.S.A.)

Table 1 (Continued) Typical Critical Depth Flumes

Reference	Type of Flume	Relevant Features	Discharge Characteristics Developed	Remarks
Inglis (11)	Standing Wave Flume	Has same sections as venturi flume. Flumes of different shapes were developed. Sometimes fitted with smooth raised floor.	Modular limit as high as 94% in cases with long gently curving sides. Empirical discharge equations and rating tables were developed.	Use of the flumes dependent on exact geometries and rating tables. Accuracy 2% if properly designed and operated.
Osborn, H.B. et al (16)	Large Critical Depth Flumes	Has broad entrance section approx. the size of approach channel, 15 ft long contracting reach and warped sidewalls, 20 ft long straight throat. Bottom slope 3% throughout.	No discharge formula presented because of varying conditions of use.	Non-standardised flume. Model studies made on each proposed location. Can handle very large flow rates.

Table 1 (Continued) Typical Critical Depth Flumes

Reference	Type of Flume	Relevant Features	Discharge Characteristics Developed	Remarks
Robinson, A.R., and Chamberlain, A.R. (20) Kruse, E.G. (14)	Trapezoidal Flumes	Has a flat-floored trapezoidal-shaped section with converging, parallel, and diverging sections.	Empirical equation developed. Modular limit 80-85%. Coefficients in equation determined experimentally.	Reasonably accurate device, particularly adapted to lined trapezoidal channels. Can handle large flow rates.
Ferguson, J.E. & Gorton, J.E. (8) Rasheed, M.A. (19)	Modified Venturi Flume	The Venturi Section is formed by introducing a curved cover over a rectangular channel. Has a rectangular throat, whose size may be varied by raising or lowering the cover. Low head loss.	Empirical equation with discharge coef. varying from 0.8 to 0.95.	Can adapt to different ranges of discharge. Has not found wide use so far in the field.

Table 1 (Continued) Typical Critical Depth Flumes

Reference	Type of Flume	Relevant Features	Discharge Characteristics Developed	Remarks
Khafagi, A (13)	Curved Entrance Venturi Flume	Flumes with different degrees of rounding in entrance section studied. Horizontal floor.	Empirical discharge equation developed; No calibration tests carried out on large size flumes.	The geometries studied were very accurate and precise. Viscous effects may be important in small flumes.
Balloffett, A. (2)	'Simple Side Construction' Flume.	Diverging section is absent. Level bottom; rectangular cross-section.	Discharge coefficients were determined for use in free flow equation.	Standard models were established for easy design and construction.
Holtan, Minshall and Harrold. U.S. Agricultural Research Service (10)	H-Flume	Operates much like a weir, but classified as flume because control section contracts from the sides. Has sloping floor.	Empirical discharge equation developed. Also specifications and calibration tables for all sizes are given. Strictly free-flow device.	Various modification of H-flume to fit specific requirements have been made. Used widely on natural streams.

Table 2

ACCURACY OF MEASUREMENTS

S. No.	Variable	Accuracy of Measurements
1	Length	± 0.001"
2	Depth Gauge	± 0.001'
3	Discharge	± 3.0%
4	Pressure Gauge	± 0.02"

TABLE 3

FLUME NO. 1

B_1 = 11.811 in. B_t = 6.142 in. L_1 = 8.504 in. L_2 = 17.008 in.

S. No.	y_1 ft	y_a ft	h_a ft	y_t ft	Q cfs	$\frac{Q^2}{g B_1^5} \times 10^4$	$\frac{Q}{\sqrt{g}\, B_t\, h_a^{1.5}}$	$\left(\frac{Q^2}{B_t^2 g}\right)^{1/3}$
1	0.090	0.087	0.086	0.073	0.0450	0.68	0.614	0.062
2	0.164	0.156	0.154	0.133	0.1140	4.30	0.650	0.116
3	0.238	0.232	0.229	0.197	0.2008	13.56	0.631	0.168
4	0.330	0.324	0.318	0.275	0.3372	38.22	0.647	0.238
5	0.416	0.408	0.397	0.354	0.4808	77.70	0.662	0.302
6	0.496	0.485	0.469	0.427	0.6377	136.70	0.684	0.364
7	0.573	0.564	0.542	0.494	0.8145	223.05	0.703	0.428
8	0.643	0.632	0.606	0.555	0.9818	324.08	0.716	0.485
9	0.745	0.736	0.699	0.649	1.2400	516.96	0.730	0.567

TABLE 4

FLUME NO. 2

	B_1 = 8.858 in.		B_t = 4.606 in.		L_1 = 6.378 in.		L_2 = 12.756 in.	
S. No.	y_1 ft	y_a ft	h_a ft	y_t ft	Q cfs	$\frac{Q^2}{g B_1^5} \times 10^4$	$\frac{Q}{\sqrt{g} B_t h_a^{1.5}}$	$(\frac{Q^2}{B_t^2 g})^{1/3}$
1	0.129	0.125	0.124	0.105	0.058	5	0.6098	0.089
2	0.228	0.221	0.219	0.189	0.142	29	0.636	0.162
3	0.327	0.319	0.315	0.277	0.260	96	0.675	0.242
4	0.430	0.427	0.412	0.374	0.398	224	0.691	0.322
5	0.538	0.528	0.505	0.472	0.567	456	0.725	0.408
6	0.632	0.633	0.596	0.556	0.742	780	0.740	0.488
7	0.739	0.738	0.693	0.676	0.968	1328	0.770	0.582
8	0.840	0.840	0.785	0.779	1.187	1996	0.783	0.667
9	0.949	0.965	0.886	0.900	1.460	3020	0.803	0.766

TABLE 5

FLUME NO. 3

B_1 = 5.906 in. B_t = 3.070 in. L_1 = 4.252 in. L_2 = 8.504 in.

S. No.	y_1 ft	y_a ft	h_a ft	y_t ft	Q cfs	$\frac{Q^2}{g B_1^5} \times 10^4$	$\frac{Q^2}{\sqrt{g} B_t h_a^{1.5}}$	$\left(\frac{Q^2}{B_t^2 g}\right)^{1/3}$
1	0.104	0.102	0.101	0.085	0.0290	9	0.619	0.074
2	0.143	0.140	0.138	0.118	0.0500	27	0.671	0.106
3	0.247	0.241	0.233	0.210	0.1136	139	0.696	0.183
4	0.385	0.378	0.359	0.336	0.2301	570	0.736	0.293
5	0.402	0.394	0.377	0.360	0.2573	712	0.765	0.316
6	0.600	0.597	0.553	0.550	0.5000	2690	0.838	0.491
7	0.800	0.810	0.728	0.774	0.8170	7181	0.905	0.682
8	0.976	1.010	0.850	0.958	1.1390	13960	1.000	0.851

APPENDIX IV

SPECIMEN COMPUTATION

APPENDIX IV

Specimen Computation

For computation purposes, the free flow discharge equation (17) is expressed as

$$G^{1/3} = R\left[X + \frac{G}{2X^2}\right] \qquad \ldots (17b)$$

where $G = \dfrac{Q^2}{g B_1^5}$

$$R = \frac{2K^{1/3} X^{2/3}}{(1 + 2K)} \qquad \text{and} \qquad X = y_1/B_1$$

Eq. (17b) may further be expressed as a polynomial of the form

$$\frac{1}{8X^6} G^3 + \frac{3}{4X^4} G^2 + \left(\frac{3}{2} - \frac{1}{R^3}\right) G + X^3 = 0 \qquad \ldots (17c)$$

For $y_1'/B_1 = X = 0.5$,

$$K = 1 - 0.29\,(y_1/B_1) = 1 - 0.29\,(0.5) = 0.855$$

$$R = \frac{2 \times (0.855)^{1/3} \quad (0.52)^{2/3}}{[1 + 2(0.855)]} = 0.453$$

Substitution of X and R in equation (17c) leads to

$$8\,G^3 + 12\,G^2 - 9.257\,G + 0.125 = 0 \qquad \ldots (17d)$$

This equation is solved with the help of a computer.

Each equation has 3 solutions - two positive and one negative. Of the two positive values for G , the lower one is adopted since it satisfies the condition F_1 is less than 1, while the higher one gives F_1 greater than 1.

The computer solution for equation (17d) is 0.01375.

APPENDIX V

MODULAR LIMIT STUDIES

APPENDIX V

Modular Limit Studies

Although critical depth flumes are designed to operate under free flow conditions, it is a common experience that they become submerged under certain operating conditions. It is thus important to know the operating condition within which the free flow equation is valid.

A limited amount of studies were conducted with flume No. 2 (B_1 = 8.858 in) in order to determine the modular limit. The tailgate was initially kept fully open to ensure free flow condition, and the upstream depth (y_1), and the tail water depth (y_2) were recorded. y_2 was measured at a fixed distance of 5 ft. downstream of the flume exit. This corresponds to a distance of about five times the maximum upstream depth. The tail gate was gradually raised, and for each y_2, the upstream depth was recorded as y_1'.

The Modular limit was then established from the plot of y_1'/y_1 against submergence ratio y_2/y_1 (fig. 20). It can be observed that the modular limit decreases with increasing discharges.

Based on the study, a modular limit of 80% is recommended for the application of the free flow equation - this value limits the increase of y_1 to 1% for the range of discharges tested.

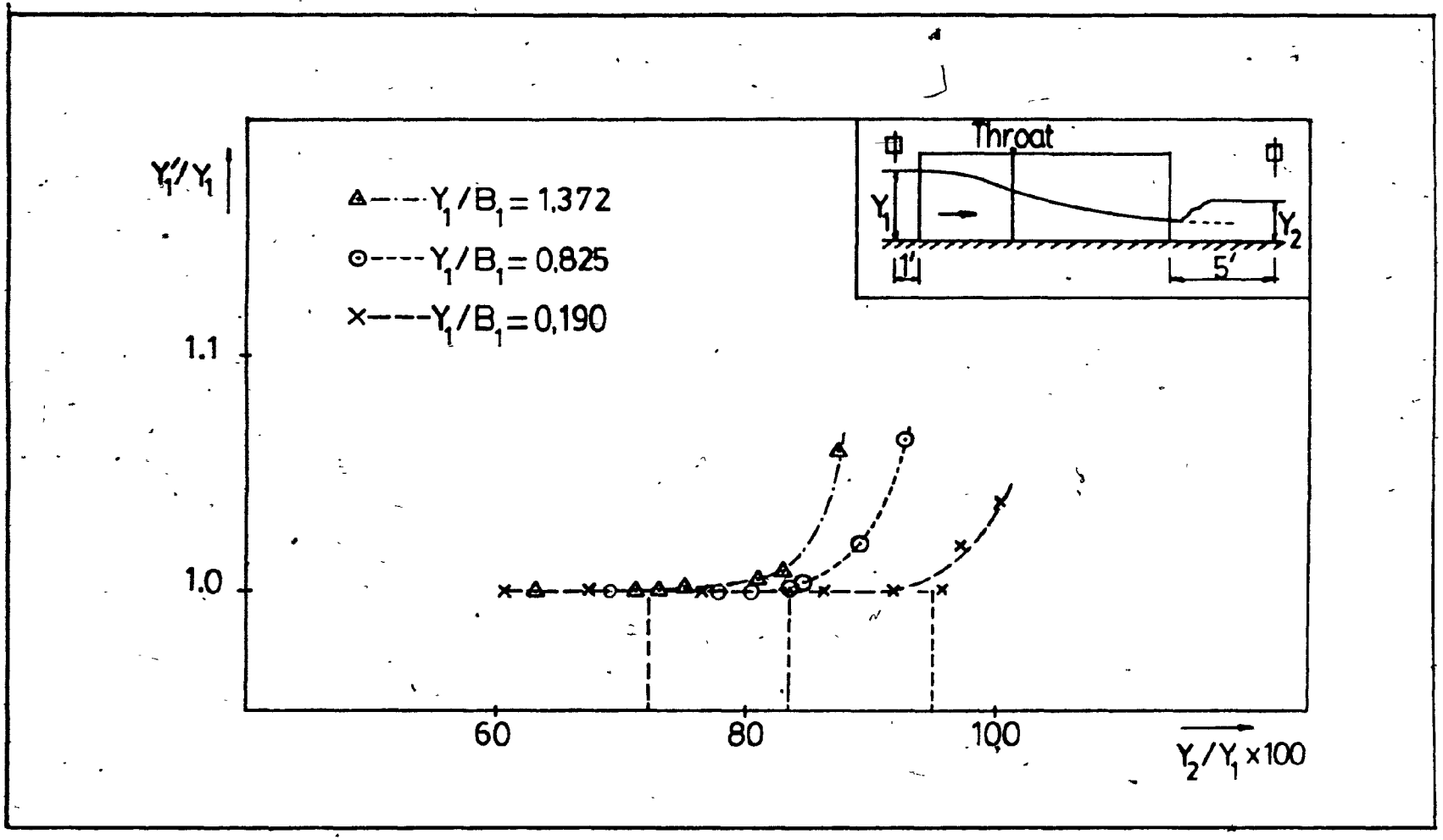

FIG. 20. VARIATION OF y_1'/y_1 WITH SUBMERGENCE RATIO y_2/y_1.

TABLE 6 MODULAR LIMIT STUDIES

FLUME 2: B_1 = 8.858 in. B_t = 4.606 in. L_1 = 6.378 in. L_2 = 12.756 in.

Q (cfs) = 1.670 y_1 (feet) = 0.609				Q (cfs) = 0.708 y_1 (feet) = 0.609				Q (cfs) = 0.067 y_1 (feet) = 0.140			
y_1'	y_2	y_2/y_1	y_1'/y_1	y_1	y_2	y_2/y_1	y_1'/y_1	y_1'	y_2	y_2/y_1	y_1'/y_1
1.013	0.254	No T.W.	Control	0.609	0.140	No T.W.	Control	0.140	0.049	No T.W.	Control
1.013	0.640	0.632	1.000	0.609	0.411	0.675	1.000	0.140	0.049	0.350	1.000
1.013	0.721	0.712	1.000	0.609	0.471	0.773	1.000	0.140	0.052	0.370	1.000
1.014	0.740	0.730	1.001	0.609	0.508	0.834	1.000	0.160	0.113	0.807	1.000
1.015	0.760	0.749	1.002	0.611	0.514	0.844	1.003	0.140	0.128	0.914	1.000
1.018	0.834	0.819	1.005	0.621	0.538	0.883	1.020	0.143	0.129	0.921	1.021
1.021	0.845	0.828	1.008	0.649	0.601	0.926	1.066	0.145	0.135	0.964	1.036
1.075	0.940	0.874	1.061								

APPENDIX VI

STUDIES ON THE EFFECT OF HUMP

APPENDIX VI

Studies on the Effect of hump:

VI-1: Theoretical Considerations:

The theoretical discharge relationship for the flow through a flume with a hump was derived by modifying eq. (16) to account for the presence of a hump. It was also assumed that both α_t and α_t^- are equal to unity. The relationship is stated below:

$$\left[\frac{Q^2}{g B_1^5}\right]^{1/3} = \left[\left(\frac{2}{3}\right)^{1.5} x\right]^{2/3} \left[\frac{y_1}{B_1} - \frac{Z}{B_1} + \frac{1}{2} \frac{Q^2}{g B_1^5} \left(\frac{B_1}{y_1}\right)^2\right] \quad \ldots (33)$$

VI-2: Experimental Verification:

Humps of heights 1.03" and 1.96" were installed in the flume and the results are shown in figs. 21 and 22. From fig. 22, it can be observe that the experimental and theoretical curves show increasing disagreement with increasing flow rates. As in the case of the flume without a hump, the streamlines were observed to have pronounced curvature in the vicinity of the throat, and the floor pressures were also observed to deviate from hydrostatic in the converging reach as well as at the throat. In one case, the hump was also installed only in the converging reach to investigate its effect on the flow. It was observed that such an action caused an even larger disagreement from theoretical analysis.

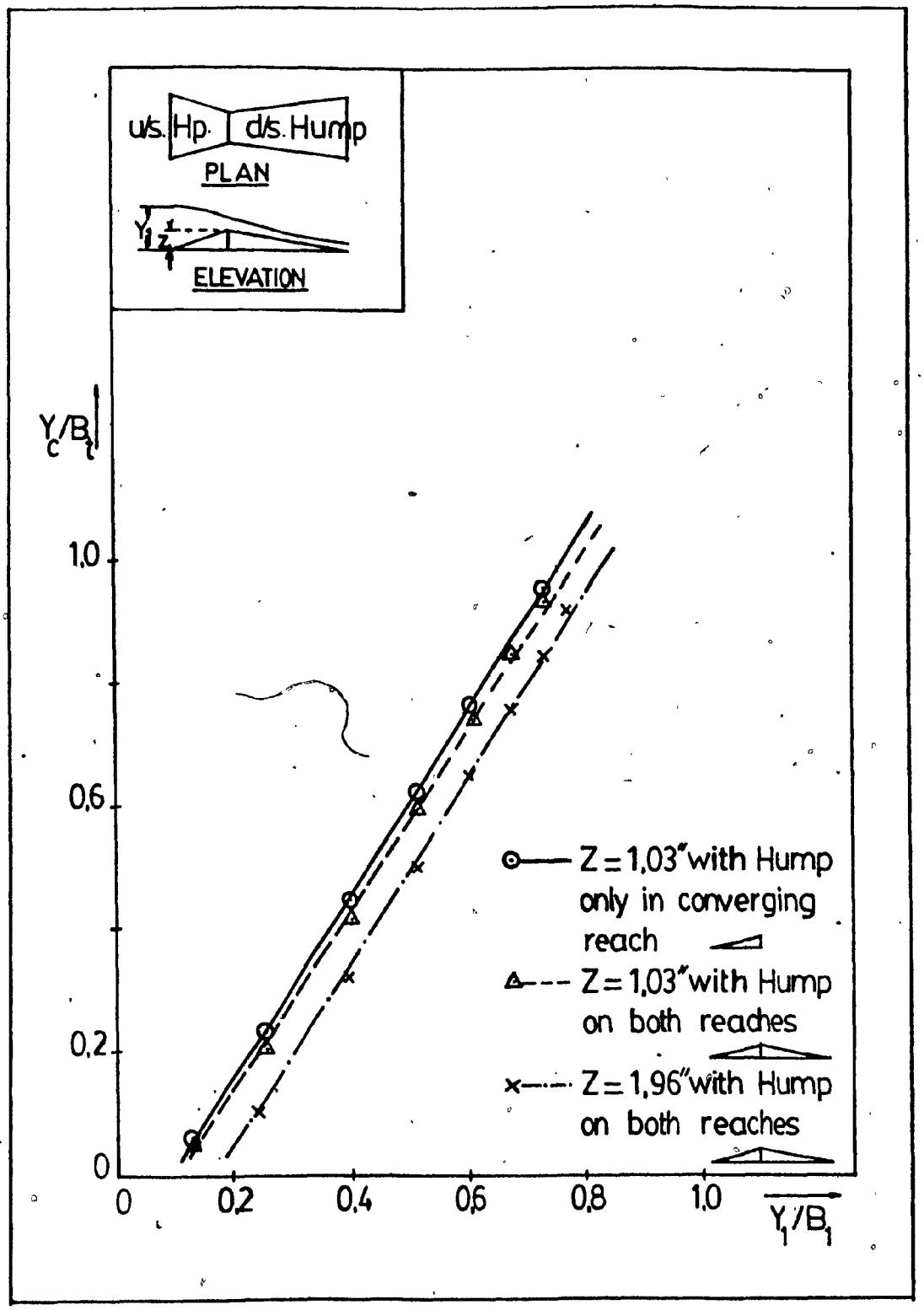

FIG. 21. FLUME WITH HUMP: VARIATION OF y_c/B_t WITH y_1/B_1.

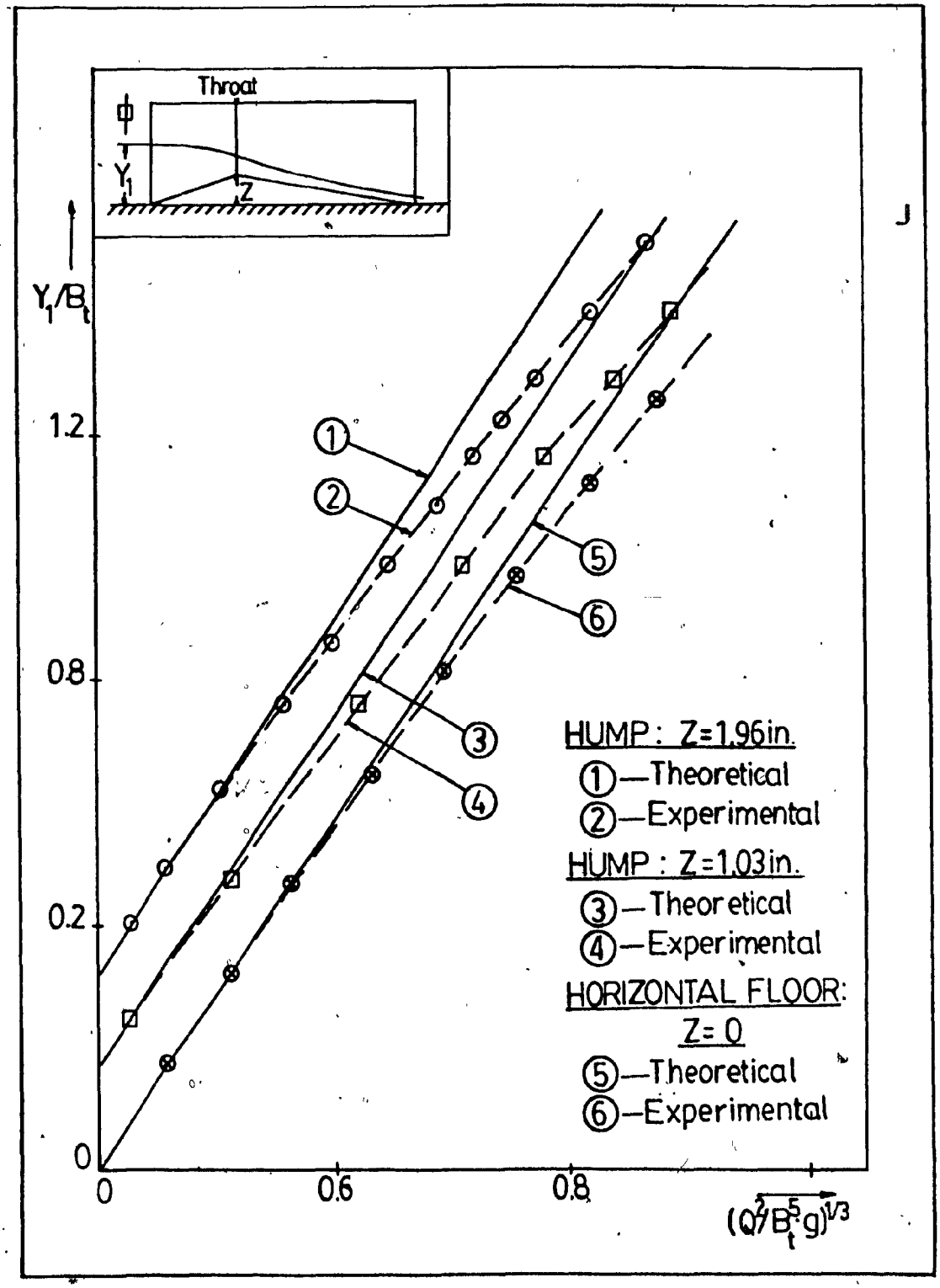

FIG. 22. FLUME WITH HUMP: VARIATION OF y_1/B_t WITH $(Q^2/B^5 g)^{1/3}$.

TABLE 7

1.03" HUMP IN CONVERGING AND DIVERGING REACHES OF FLUME

FLUME 1: B_1 = 11.811 in. B_t = 6.142 in. L_1 = 8.504 in. L_2 = 17.008 in. Z = 1.03 in.

S. No.	y_1 ft	y_t ft	Q cfs	$y_c = \left(\frac{Q^2}{g B_t^2}\right)^{1/3}$ ft
1	0.127	0.034	0.0114	0.025
2	0.245	0.125	0.1006	0.106
3	0.389	0.248	0.2871	0.214
4	0.504	0.348	0.4900	0.305
5	0.596	0.431	0.6785	0.379
6	0.661	0.491	0.8325	0.435
7	0.717	0.537	0.9626	0.479

TABLE 8

1.03" HUMP IN CONVERGING REACH OF FLUME

FLUME 1: B_1 = 11.811 in. B_t = 6.142 in. Z = 1.03 in. L_1 = 8.504 in. L_2 = 17.008 in.

S. No.	y_1 ft	y_t ft	Q cfs	$y_c = \left(\frac{Q^2}{g B_t^2}\right)^{1/3}$ ft
1	0.127	0.022	0.0138	0.028
2	0.245	0.111	0.1147	0.116
3	0.389	0.236	0.3133	0.227
4	0.504	0.338	0.5208	0.318
5	0.596	0.420	0.7051	0.389
6	0.661	0.486	0.8765	0.450
7	0.717	0.538	1.0235	0.499

TABLE 9

1.96" HUMP IN CONVERGING AND DIVERGING REACHES OF FLUME

FLUME 1: B_1 = 11.811 in. B_t = 6.142 in. L_1 = 8.504 in. L_2 = 17.008 in. Z = 1.96 in.

S. No.	y_1 ft	y_t ft	Q cfs	$y_c = \left(\frac{Q^2}{g B_t^2}\right)^{1/3}$ ft
1	0.234	0.056	0.035	0.053
2	0.388	0.177	0.195	0.165
3	0.504	0.274	0.378	0.257
4	0.596	0.355	0.555	0.332
5	0.661	0.414	0.700	0.387
6	0.717	0.464	0.826	0.432
7	0.759	0.502	0.935	0.470